TECHNISCHE UNIVERSITÄT WIEN

D I P L O M A R B E I T

Hard- and software development of a mechanobiological organ-on-a-chip platform

Ausgeführt am Institut für

Angewandte Synthesechemie

der Technischen Universität Wien

unter der Anleitung von

Univ.Prof. Dipl.-Ing. Dr. Peter Ertl

durch

Selina Schweinberger

Datum

Unterschrift (Student)

Die approbierte gedruckte Originalversion dieser Diplomarbeit ist an der TU Wien Bibliothek verfügbar
The approved original version of this thesis is available in print at TU Wien Bibliothek.
TU Bibliothek Your knowledge hub WIEN

Master thesis

Hard- and Software Development of a mechanobiological Organ-on-a-Chip Platform

ausgeführt unter der Leitung von

Univ. Prof. Dipl.-Ing. Dr. Peter Ertl
E163/E164 Institut für Angewandte Synthesechemie
Technische Universität Wien

und
Dr. Barbara Eva Maria Bachmann MSc.
Institut für Angewandte Synthesechemie
Technische Universität Wien

von

Selina Schweinberger, BSc
Masterstudium Biomedical Engineering
11715700

Wien, 2021

Die approbierte gedruckte Originalversion dieser Diplomarbeit ist an der TU Wien Bibliothek verfügbar
The approved original version of this thesis is available in print at TU Wien Bibliothek.
TU Bibliothek Your knowledge hub WIEN

Abstract

While mechanobiological research interfaces biology and engineering, most current systems still rely on an expensive and bulky periphery to relay pressure to and from pneumatic valves to a cell-culture device. Such a periphery usually consists of a pressure system, pumps, and a computer for control. However, setting up such a system may require engineering expertise or commercial solutions. Here, a platform is presented, which allows scientists to perform dynamic cultivation for biology experiments on microfluidic devices to facilitate mechanobiological research at low cost. The platform consists of an Arduino based controller paired with a transistor array which can drive eight solenoid valves simultaneously. The pneumatic of the platform is controlled by a LCD and rotary encoder, while encased into a custom-made housing. The footprint of the system is 6.5 x 9 x 13 cm and the total material price is less than 100 €. As a demonstration, we show that the platform is capable of automatically inducing reproducible wounds on a wound healing chip.

Die approbierte gedruckte Originalversion dieser Diplomarbeit ist an der TU Wien Bibliothek verfügbar
The approved original version of this thesis is available in print at TU Wien Bibliothek.
TU Bibliothek Your knowledge hub WIEN

Acknowledgements

It would not have been possible for me to design and built this product, if it weren't for the support of several people. I received complete trust and generous support form every single person in the research group of Univ. Prof. Dipl.-Ing. Dr. Peter Ertl. Highlighting Prof. Ertl who encouraged me throughout my time, not only with my thesis but also with my future career. I have learned so much in this time. Not only about the field of microfluidics and la-on-a-chip technologies but also about university research. They had always time for me and my questions and supported me in the best way possible. Every shared beverage or snack was pleasant and made me want to stay longer.

I would especially like to thank my supervisor Barbara Bachmann MSc. for her patience and support, as well as for teaching me all the things I did not know about cells - which was a lot. Besides giving me helpful answers to my questions, I really enjoyed speaking dialect with you. Special thanks to Florin Metzler MSc. who kindly listened to my endless seaming talks and worries and always believed in me. To all the people who have been there for me and given me advice and a healthy work-life balance, thank you. Thank you all for helping me achieving my diploma.

Die approbierte gedruckte Originalversion dieser Diplomarbeit ist an der TU Wien Bibliothek verfügbar
The approved original version of this thesis is available in print at TU Wien Bibliothek.
TU WIEN Bibliothek Your knowledge hub

Contents

Abstract **I**

Acknowledgements **II**

List of Figures **V**

List of Tables **VI**

Acronyms **VII**

1 Introduction **1**

1.1 Organ-on-a-chip 2

1.2 Biomechanical cues in organ-on-a-chip systems 4

1.2.1 Flow/shear systems 5

1.2.2 Stretching systems 5

1.2.3 Compressive load 6

1.3 Engineering a mechanobiological platform 6

1.3.1 Bioreactor design requirements 7

1.4 Pneumatics in microfluidic devices 9

1.4.1 Pneumatic control systems 9

1.4.2 Pumping in microfluidics 11

1.5 Aim of the thesis 13

2 Materials and Methods **14**

Die approbierte gedruckte Originalversion dieser Diplomarbeit ist an der TU Wien Bibliothek verfügbar
The approved original version of this thesis is available in print at TU Wien Bibliothek.
TU Bibliothek Your knowledge hub WIEN

2.1 Pneumatic system design 14
2.2 Electronic subsystem and evaluation 14
2.3 Additive manufacturing 16
2.4 Programming 16
2.5 Experimental set-up 17
2.6 Cell culture 18
2.7 Imaging 19
2.8 List of materials 20

3 Results **23**
3.1 System periphery to facilitate biomedical implementation 23
3.1.1 Housing optimization 24
3.1.2 Microcontroller-based electronic system design 29
3.2 Software implementation 34
3.3 Bill of materials 37
3.4 Operation instructions 37
3.5 Validation and characterization of the platform 39
3.5.1 Effect of compressive stress on dermal fibroblasts 40

4 Discussion **43**

References **46**

A Appendix **54**
A.1 Design for a upscaled platform 54
A.1.1 Schematic 55
A.2 Parts list 56

Die approbierte gedruckte Originalversion dieser Diplomarbeit ist an der TU Wien Bibliothek verfügbar
The approved original version of this thesis is available in print at TU Wien Bibliothek.
TU Bibliothek Your knowledge hub WIEN

List of Figures

1.1 Organ-on-a-Chip Design 3
1.2 Mechanobiological Cues in the Microenvironment 4
1.3 Schematic of a Mathies Valve 10
1.4 Schematic of a Solenoid Valve 11

2.1 Pin Diagram Arduino Uno Rev3 15
2.2 Chipdesign 18

3.1 Electro-pneumatic System Design 24
3.2 Bottom Part Details 25
3.3 Middle and Top Part Details 26
3.4 Middle and Top Part of the Platform 27
3.5 Assembled mechanobiological Organ-on-a-Chip platform 28
3.6 Equivalent circuit of a solenoid valve 30
3.7 Logic Diagram of the ULN2803a 32
3.8 Solenoid circuit with UI 33
3.9 Graphical User Interface 34
3.10 Program flow 36
3.11 Experimental set-up 39
3.12 Wound healing biochip 40
3.13 Close-up of the microchannel 41
3.14 Cell viability on the wounded biochip 42

Die approbierte gedruckte Originalversion dieser Diplomarbeit ist an der TU Wien Bibliothek verfügbar
The approved original version of this thesis is available in print at TU Wien Bibliothek.
TU Bibliothek Your knowledge hub WIEN

List of Tables

2.1 List of Materials 20

3.1 Driver comparison 30

3.2 Bill of Materials - Platform only 38

A.1 Part List for Upscaled Version 56

Die approbierte gedruckte Originalversion dieser Diplomarbeit ist an der TU Wien Bibliothek verfügbar
The approved original version of this thesis is available in print at TU Wien Bibliothek.
TU WIEN Bibliothek Your knowledge hub

Acronyms

BJT Bipolar Junction Transistor. 29

DMEM Dulbecco's Modified Eagle Medium. 18

DPBS Dulbecco's Phosphate-Buffered Saline. 17, 19

ECM Extracellular Matrix. 4

FCS Fetal Bovine Serum. 18

FDM Fused Deposition Modelling. 16

GPIO General Purpose Input/Output. 31

GUI Graphical User Interface. 34, 37

HDF Human Dermal Fibroblasts. 18, 41

IDE Integrated Development Environment. 16, 37

IGBT Insulated-gate Bipolar Transistor. 29

LCD Liquid Crystal Display. 16, 24, 37

MOSFET Metal Oxide Semiconductor Field Effect Transistor. 29

PCB Printed Circuit Board. 33

PDMS Polydimethylsiloxane. 8, 17, 39

PEI Polyetherimide. 16

PLA Polyactic Acid. 16

PVC Polyvinyl Chloride. 14, 18

Die approbierte gedruckte Originalversion dieser Diplomarbeit ist an der TU Wien Bibliothek verfügbar
The approved original version of this thesis is available in print at TU Wien Bibliothek.
TU Bibliothek Your knowledge hub WIEN

UI User Interface. 16, 18, 26, 34

VDC Volts of Direct Current. 14

Die approbierte gedruckte Originalversion dieser Diplomarbeit ist an der TU Wien Bibliothek verfügbar
The approved original version of this thesis is available in print at TU Wien Bibliothek.
TU WIEN Bibliothek Your knowledge hub

1. Introduction

The relationship between cells, the extracellular matrix and their environment is of strong interest to better understand human diseases in biomedical research. Mammalian cells inhabit all tissues of the human body and are essential for proper tissue development and maintenance. Cell fate and development are, amongst others, regulated through mechanical cues. For stem cells, intrinsic and extrinsic forces regulate development, homeostasis and regeneration.[1] The behaviour of cells during biological processes, including cell migration and morphological changes, strongly depends on external mechanical influences. This mechanical information is provided by the cells' extracellular environment.[2]

Recently, it has become well established that a wide understanding on cellular processes and pathologies can be gained by adding a different parameter, in this case, mechanical forces to biomedical research models. These mechanical influences are then translated into biochemical signals, a process called mechanotransduction. It is important to clarify cell function through better understanding of physiological processes. A goal is to mimic in *vitro* physiological processes. The ability of cells to respond to force and physical environment is what influences their shape, mobility and differentiation.[3] The cellular response to a mechanical stimulus affects the overall function of a multicellular system, which is critical for both, physio- and pathological tissue- and organ models.[4]

Disruptions in these sensing mechanisms/functions have been implicated in several diseases such as osteoporosis, cardiovascular diseases, and osteoarthritis. This interdisciplinary field spanning from biology to computational mechanics is termed mechanobiology. Mechanobiology refers to every aspect of cell biology, in which physical forces occur. No matter if the forces are sensed, imprinted, generated, or led to alterations in function.[5]

Understanding the underlying principle of mechanotransduction and the resulting cellular response is a major challenge. The most promising method to address this challenge is to mechanically stimulate living cells and tissues and then assess their response. Although mechanobiology research is thriving, it is still limited by the available techniques to impose a mechanical stimulus.[6]

Die approbierte gedruckte Originalversion dieser Diplomarbeit ist an der TU Wien Bibliothek verfügbar
The approved original version of this thesis is available in print at TU Wien Bibliothek.
TU Bibliothek Your knowledge hub WIEN

This thesis aims at designing and implementing a platform to facilitate mechanobiological organ-on-a-chip research. The successfully established "MechanoTron" will allow scientists to precisely control mechanical input on cell layers and assemblies to assess cellular responses to compression or stretching. The following chapter will summarize technical platform design details and manufacturing processes to set a theoretical framework for the described experimental work.

1.1 Organ-on-a-chip

The microfluidic cell culture technology, often referred to as organs-on-a-chip, recapitulates the key functional aspects of organs and tissues for more physiological relevance.[7–9] Understanding the physiology of the human body begins with understanding each individual element. To fully understand the pathophysiology and formation of tissues and organs, it is crucial to study the cells behaviour in context to each other, as a highly dynamic three-dimensional (3D) structure.[8] Modelling and testing of human derived cells in a 3D construct offered a more predictive assessment of a human response in a physiological environment. Nevertheless, the lack of important physiological conditions, such as the application of mechanical stimuli or a diffusion gradient could not be applied to embedded 3D constructs. By combining 3D cell culture techniques and microfluidics, more physiological relevant models can be cultivated.

Organ-on-a-chip offers key advantages of directly influencing the phenotype and behaviour of living cells, as well as the integration of gradients, implementation of fluid flow and vascularization.[8] Defined, micrometre-sized channels enable to reconstruct 3D tissue architecture and reduce material consumption and costs. Because of the small dimensions provided by the on-chip-technology, material and the resulting material cost is reduced. Primary human cells needed to gather pharmaceutically relevant data are scarce and require elaborate cell isolation techniques. Microfluidic technology leads to cost reduction by down-scaling needed cell numbers and expensive consumables. The implementation of microengineering methods to construct cell-based microfluidic cultures has led to considerable progress by enabling to tailor the cellular microenvironment in vitro. Current organ-on-a-chip systems include lung, kidney, and vasculature-on-chip systems, which rely on dynamic cultivation for proper function.[14]

However, the application of mechanical cues to tissues and organs-on-a-chip remains a challenge. So does the industrial producibility. Manually produced academic proof-of-concept prototypes are not scalable for industrial manufacturing. The problem hereby is the production of the biochips. Because most organ-on-a-chip devices are fabricated with soft lithography, which is not applicable for industry due to its time intensive and expensive production.[15]

Die approbierte gedruckte Originalversion dieser Diplomarbeit ist an der TU Wien Bibliothek verfügbar
The approved original version of this thesis is available in print at TU Wien Bibliothek.
TU Bibliothek Your knowledge hub WIEN

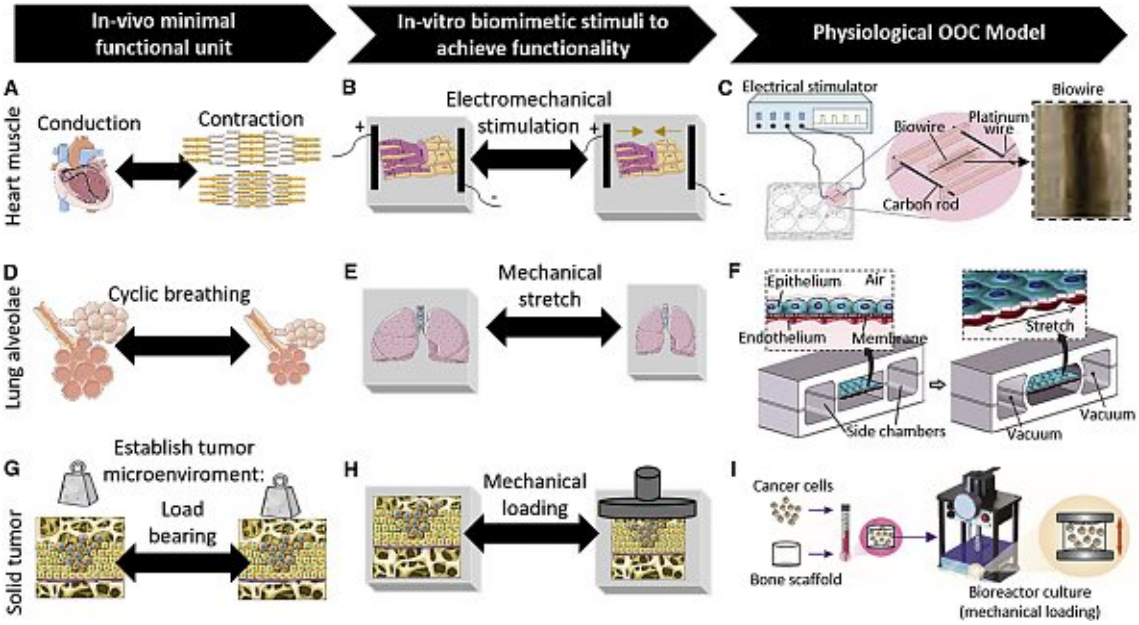

Figure 1.1: Organ-on-a-Chip Design
The design considerations for organ-on-a-chip systems involves mimicking the in vivo stimulation. (A-C) An example for a heart muscle model using cardiac tissue and electromechanical stimulation.[10] (D-F) Design configurations of lung alveolae on-a-chip. Cyclic breathing is mimicked by mechanical stretching of the membrane.[11] (G-I) Solid tumor model using mechanical loading to achieve in vitro functionality. The cancer cells are embedded in a bone scaffold which is cyclically compressed in a mechanically loaded bioreactor.[12] Figure from [13].

Die approbierte gedruckte Originalversion dieser Diplomarbeit ist an der TU Wien Bibliothek verfügbar
The approved original version of this thesis is available in print at TU Wien Bibliothek.
TU Bibliothek Your knowledge hub WIEN

1.2 Biomechanical cues in organ-on-a-chip systems

Organ-on-a-chip systems can apply mechanical forces to cell cultures via perfusion (shear stress), stretching, and compression (Figure 1.2).[16] These mechanical stimuli represent physiologic dynamic phenomena such as blood flow, inhalation, or cartilage compression. Alternatively, mechanical forces can be used to generate pathological scenarios like skin wounds via compression of cell layers. [17–19]

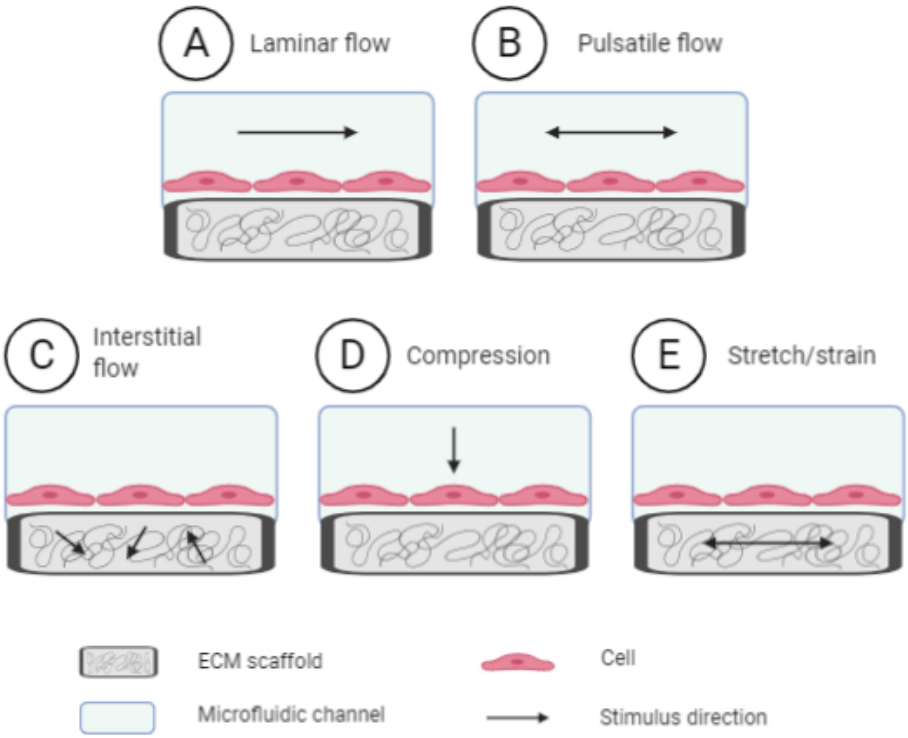

Figure 1.2: Mechanobiological Cues in the Microenvironment
A simplified visualization of a microfluidic channel with an Extracellular Matrix (ECM) scaffold and cell lining. The black arrow represents the stimulus direction. The stimulation strategies for microfluidic 2D/3D cell cultures include (a) Laminar and (b) Pulsatile flow, which generate shear stress on the cell surface. Whereas (c) Interstitial flow through the ECM generates shear stress to the cells attached to the scaffold. (d) Compressional force on is generated on top of the cell by compression. Stretching of the scaffold (e) yields to mechanical strain to the attached cell. Figure adapted from [4].

Die approbierte gedruckte Originalversion dieser Diplomarbeit ist an der TU Wien Bibliothek verfügbar
The approved original version of this thesis is available in print at TU Wien Bibliothek.
TU Bibliothek Your knowledge hub WIEN

1.2.1 Flow/shear systems

Fluid shear stress is among the most important mechanostimuli, as it occurs naturally in various physiological conditions.[20] Multiple developmental processes, such as blood vessel formation, rely on shear stress to guide cell differentiation.[21–23] Arguably, shear stress affects the cardiovascular system the most, as the fluid environment near arterial branches is distinct from the laminar pulsation flow dynamics present in straight sections of the vessels.[24]

Microfluidic systems can recreate different flow types governing cellular behavior in vivo. For example, shear stress is in microfluidic devices is generally generated by external pumping via syringe pumps or integrated micropumps. Flow in microfluidic channels is always laminar due to reduced diameters resulting in small Reynolds numbers (Figure 1.2a).[25] While laminar flow has been commonly used in various microfluidic systems, for example in the formation of small blood vessels-on-a-chip [26], a pulsatile flow is encountered in larger blood vessels, as the beating heart pumps blood through the body (Figure 1.2a). This pulsatile flow can be mimicked using peristaltic pumps.

The fluid flow through or around a 3D ECM is called interstitial flow. It differs greatly from open-channel flow by generally having a slower flow rate and a multi-directional flow through and across the matrix (Figure 1.2c).[4]

1.2.2 Stretching systems

Physiological altering of cells as a response to mechanical strain is a well-known phenomenon. There are two prominent ways of applying tensile stress on cells: cultivating cells back-to-back on cyclically stretched membranes and cultivating cells directly on a deflecting membrane.[27] The first method was developed for a lung-on-a-chip model by Huh et al.[11] and has since inspired many scientists to investigate a variety of models. The developed system consists of a flexible membrane which is stretched by vacuum channels on either side of the cultivating chamber.[11]

The second approach exerts stretching to cultured cells by inflating the underlying membrane on which the cells are being cultured.[27] This method also allows for cyclic actuation, which among others has been used to model muscular dystrophy on a chip.[28] Uniaxial stretchable substrates enable the mechanical stimulation of cells (contraction) as well as a biomimetic relaxation phase and are widely reported to align cells.[29–33]

Die approbierte gedruckte Originalversion dieser Diplomarbeit ist an der TU Wien Bibliothek verfügbar
The approved original version of this thesis is available in print at TU Wien Bibliothek.
TU Bibliothek Your knowledge hub WIEN

1.2.3 Compressive load

Dynamic compression is a useful tool for biomechanics as it shows the interplay between mechanical forces and the health and function of the tissue. Mechanical forces are an essential part of the environment for cartilage, as it is a mechanically robust tissue that distributes loads and resists compression.[34]

Compression on cells can be realized by either positive or negative pressurization and has established itself by its simplicity and ease of use. Despite their versatility and adaptability, compression systems in organ-on-a-chip research have only improved incrementally within the last decade. Essentially, the compressive load system is designed to compress air or liquid to a planar surface. Compressive load applies force along a single axis either above or below the compressed object.[35]

Positive is the versatility and adaptability these methods offer. Compression can be achieved by either vacuum or positive pressure and frequency and/or pressure can be changed easily to mimic physiological behaviour. A deflected membrane can press on a cell covered surface with different pressures, thus yielding different results. With low pressures and repeated membrane deflection, differentiation of stem cells can be stimulated.[36] By inducing high pressure for a short amount of time, this system can be used for wounding of a cell migration assay.[37]

1.3 Engineering a mechanobiological platform

An important goal of tissue and organ-on-a-chip research is to develop physiological relevant models with miniaturized biological instruments (chip format). One common feature for mechanobiology-on-chip systems is that they all require a method of force application. Therefore, access to a system or platform is essential. This system must be comparable to conventional manual methods to achieve automated mechanobiological research. In the past, pneumatically driven microfluidic chips have been introduced. These chips can require the connection of dozens of tubes for actuation and reagent supply and are dependent on mostly bulky periphery such as compressed pressure sources and computers. Pressure lines are either controlled by computers or entirely operated manually. This bulky and inconvenient periphery severely limits the progress of automatization and parallelism in mechanobiological research.[38]

Darling and Athanasiou named any manufactured device or system that uses means to influence biological processes, bioreactor.[39, 40] In context with cells, it usually refers to a device or system designed to grow or manipulate/ investigate a cell culture. Bioreactors used for tissue engineering differ vastly form common industrial bioreactors, as it attempts to simulate a physiological environment. Hereby,

Die approbierte gedruckte Originalversion dieser Diplomarbeit ist an der TU Wien Bibliothek verfügbar
The approved original version of this thesis is available in print at TU Wien Bibliothek.
TU Bibliothek Your knowledge hub WIEN

promoting cell or tissue growth *in vitro*.

In vivo, the forces experienced by tissues and cells vary in type and magnitude, depending on the physical location.[41] Thus, each tissue (blood vessel, cartilage, bone, etc.) has different requirements, making the design and build of a bioreactor complicated. Bioreactors perform at least one of the following functions: (1) provide spatially uniform cell distribution, (2) maintain desired composition of gases and or nutrients in culture medium, (3) facilitate mass transport to the tissue, (4) induce signals (i.e. chemical / mechanical) to provoke mechanisms or (5) provide information about the formation of the tissue structure.[40–44]

Common approaches are to either use a commercially available bioreactor or, to use an application specific, manual operated system.[45–47] The cost of a commercial bioreactor quickly adds up to thousands of euros with the additional drawback of a bulky build. The disadvantage of a custom build system is that it requires technical knowledge to assemble and manage the pneumatic apparatus.

1.3.1 Bioreactor design requirements

Microfluidic platforms provide the opportunity to down-scale conventionally bulky bioreactors to a object slide-sized microfluidic system in the form of biochips and organ-on-a-chip systems.[40, 43] As a cell culture in some cases requires induced signals (shear/tensile stress, compression) for an accurate *in vitro* representation, a platform is needed. The design of a bioreactor should be as simple as possible, avoiding machined recesses and overengineering. Simplicity is key, as this platform should be accessible with limited training. A quick way to connect and disconnect or in some cases assemble the bioreactor is important. Apart from being more efficient, this also reduces the time cell-seeded constructs spent outside the incubator. Thus, minimizing negative impacts of environmental changes on cell behavior and guaranteeing stable measurement conditions.[40]

The detailed requirements for a bioreactor design are application and/ or tissue specific, but the few general principles stated above must be followed, regardless of the resulting application. The specific application must be kept in mind during the design process to ensure all design constraints are met.[40]

Any design involving fluids, leakage in seals rises serious issues. A good design should decrease the number of seals, thus preventing further problems. If a bioreactor is being designed, it may be worth thinking about upscaling. This may mean designing a device that is relatively easy to enlarge without many changes (adaptability) or designing a device that can easily be replicated.[40]

The types of bioreactors are categorized by their most prominent characteristics. Compression bioreactors are widely used in cartilage engineering as they are able

Die approbierte gedruckte Originalversion dieser Diplomarbeit ist an der TU Wien Bibliothek verfügbar
The approved original version of this thesis is available in print at TU Wien Bibliothek.
TU Bibliothek Your knowledge hub WIEN

to apply a static and/ or dynamic load. The load bearing objects are usually flat plates, as they distribute the load evenly, or flexible PDMS membranes/balloons which expand.[48] The compression forces fluids from the compressed area into interstitial spaces, thereby generating shear stress and strain. This makes a compression bioreactor especially useful for experiments regarding the musculoskeletal system. It is a widely used tool for bones and cartilage, as they are very sensitive to compression forces.[39, 40, 49–55]

Strain bioreactors are used when tendons, ligaments, bones, cartilage, or cardiovascular tissue is modelled. The system design can be very similar to compression bioreactors, only differing in the force-transferring system. For microfluidics, the most common method of force transfer is either a microfabricated membrane on which cells are cultured and then mechanically stretched or a microfluidic device that includes in addition to the microfabricated membrane an ultra-thin, porous membrane used as an *in vitro* barrier.[56] Although there is a commercially available stretching platform available for over 30 years (Flexcell International Corp. [57]), there is none for microfluidic chips. Therefore many research groups design their own platform for microfluidic applications.

Flow perfusion bioreactors generally consist of a pump connected (by tubing) to a scaffold chamber. A fluid pump continuously forces media through the cell-seeded scaffold thus enhancing fluid transport. An advantage is the ease in media replacement through the media reservoir. A challenge is optimizing the flow rate and the balance between mass transfer of nutrients and waste products to and from the cells.[40, 41]

Available Bioreactors

Currently there are only a few commercially available bioreactors, which allow mechanical stimulation of a cell-seeded constructs. The available options are stimulation specific bioreactors. Flexcell International Corp. [57] offers a cell stretching system form Strex Systems [58] while a bioreactor with multi - axial capabilities such as torsion and tension is marketed by TA Instruments. [59] Besides commercially available systems, several customized mechanical stimulation systems have been reported in recent years.[38, 60–62] Although they offer translatability, they are specific to one application.

Die approbierte gedruckte Originalversion dieser Diplomarbeit ist an der TU Wien Bibliothek verfügbar
The approved original version of this thesis is available in print at TU Wien Bibliothek.
TU Bibliothek Your knowledge hub WIEN

1.4 Pneumatics in microfluidic devices

Microfluidic technologies allow the precise control of small amounts of fluid through channels at a sub millimetre-scale.[62] Microvalves are a useful tool in microfluidic devices, as they not only allow precise flow control regardless of the medium, but they also allow peristaltic pumping.[63] The most common method of actuation is a mechanically movable membrane to open or close the orifice, thus preventing or allowing flow. In terms of fabrication, microvalves are usually fabricated with MEMS- based bulk or surface micromachining technologies.[63]

The commonly used micromechanical valve is known as Quake valve. It enabled applications in the several fields, including single cell analysis [64], hydrogel engineering [65], complex fluid handling systems and on-chip tissue and organ engineering.[62, 66] The Quake-style valve is a monolithic soft polymer valve which uses pneumatic actuation to control channels and manipulate the fluid wall.[67, 68]

Quake valves allow the fabrication of high-density array systems, due to their small footprint and their compatibility with the soft-lithography technology. Nonetheless, an external (off-chip) actuation system is required. This usually consists of computer controlled pneumatic actuators (valves), a control unit (computer) and a gas distribution system.[69] A system of solenoid valves is typically used to control the pressure applied to the chip.

Pneumatic valves can be designed to either actuate-to-open or actuate-to-close. While Quake valves are normally closed (actuate-to-close) valves, normally closed valves typically utilize a vacuum for actuation.[70] The Mathies valve consists of three to four layers of glass and PDMS rather than just PDMS. The vacuum is applied in displacement chambers and actuates the PDMS membrane to open the fluid layer. This is shown in Figure 1.3. Mathies valves are primarily used for applications that require clear devices for imaging techniques.[71, 72]

1.4.1 Pneumatic control systems

Valves are mechanical devices that regulate, control, or direct the flow or pressure in a system by opening or closing. They are the essential components for hydraulic or pneumatic systems for they convey liquid and gases. Besides the widespread applications in piping systems, the ability to manipulate fluid flow in microfluidics established (micro-)valves in a new field.

Solenoid valves can be categorized by their initial state (normally open/ normally closed), controlled medium, powering electric current characteristics, and generated field strength. The mechanisms vary from pilot operated to direct acting valves.

Die approbierte gedruckte Originalversion dieser Diplomarbeit ist an der TU Wien Bibliothek verfügbar
The approved original version of this thesis is available in print at TU Wien Bibliothek.
TU Bibliothek Your knowledge hub WIEN

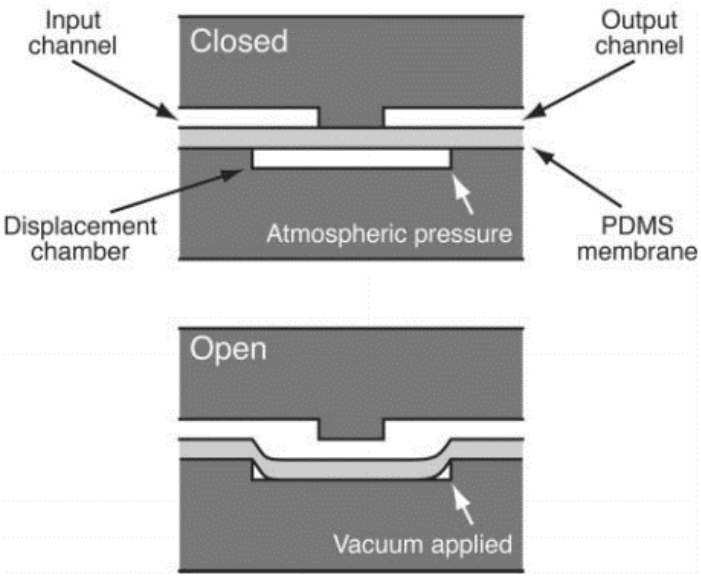

Figure 1.3: Schematic of a Mathies Valve
The valve consists of a PDMS layer in between two glass layers. A vacuum applied through the displacement chamber actuates the PDMS layer thereby opening the fluid channel. Figure from [70].

The valve can use a two- port design to regulate single flow, or use a three or more port design for intended switch flows. A manifold can be used for multiple solenoids, in which case the solenoids are either body-ported or base-mounted.

Solenoid valves are electrically operated and therefore automatic valves. Because of the automatic operation, they are commonly used to replace manual valves or as a remote control element. Solenoids operate using an electromagnetic coil to change the state of a valve - fully open to fully closed, or vice versa.

One of the advantages of solenoid valves is their fast response time, which allows use in several applications including: (1) reducing torque on the engine in compressors, (2) irrigation systems in agriculture, and (3) as a safety measurement in industrial presses, where a failure of the solenoid could harm the operator. In such case, 3/2 - way solenoid valves are used, as they are equipped with a double valve system, allowing failure of one of them.[73] Solenoid valves consist of a coil, plunger, and sleeve assembly, as can be seen in Figure 1.4.

Various types of solenoid valves are commercially available, but the main variants are either pilot operated or direct acting. Pilot valves use a plunger or system pressure to open and close the main orifice (see number 7 and 9 in Figure 1.4, respectively) in the valve body, by raising or lowering the plunger within a sleeve tube by the coil.

Die approbierte gedruckte Originalversion dieser Diplomarbeit ist an der TU Wien Bibliothek verfügbar
The approved original version of this thesis is available in print at TU Wien Bibliothek.
TU WIEN Bibliothek Your knowledge hub

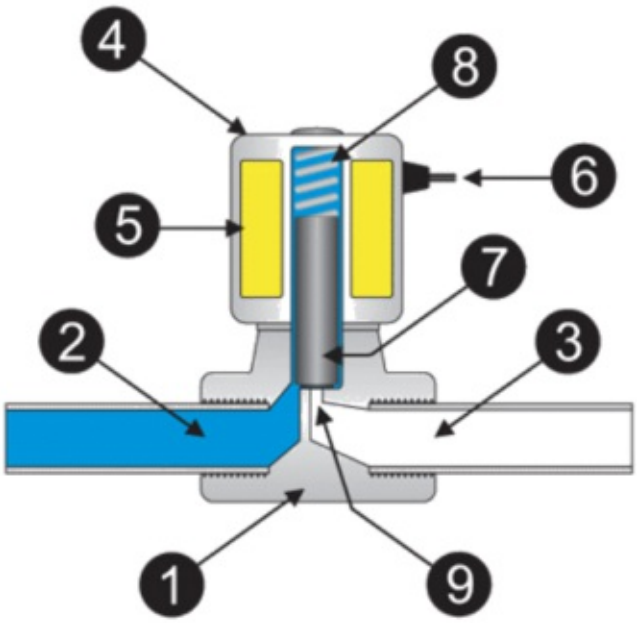

Figure 1.4: Schematic of a Solenoid Valve
1. Valve Body 2. Inlet Port 3. Outlet Port 4. Coil / Solenoid 5. Coil Windings 6. Lead Wires 7. Plunger 8. Spring 9. Orifice. Figure from [74].

Directly acting solenoid valves are used in systems with low flow capacities or systems with a pressure differential across the valve orifice.[74, 75] Solenoid valves are either normally closed or normally open. In normally closed valves, a spring (number 8 in Figure 1.4) holds the plunger against the orifice and thus prevents flow.[76] If the solenoid coil (number 5 in Figure 1.4) gets energised, the resulting magnetic field raises the plunger to enable flow.

In case of an absence of the solenoid excitation, the spring returns to its neutral (closed end) position and the valve is kept close. In case of a normally open valve, the orifice gets sealed by the plunger when the coil is energised. Solenoid valves are the most frequently used control elements in fluidics and are known for their high reliability, long service life, low control power and compact design. They offer fast and safe switching at a low price.

1.4.2 Pumping in microfluidics

There are several mechanisms for pumping in microfluidics: surface tension, pressure driven, osmosis, capillary, gravity driven, hydrostatic pressure and vacuum.[77] Pumping and manipulating the small fluids volumes in microfluidic systems can require additional infrastructure for example (macroscale) pumps, pressure/vacuum, and valves.[78] For integrated micropumps, a small size is a key aspect. Whereas

Die approbierte gedruckte Originalversion dieser Diplomarbeit ist an der TU Wien Bibliothek verfügbar
The approved original version of this thesis is available in print at TU Wien Bibliothek.
TU Bibliothek Your knowledge hub WIEN

these aspects are less important for external syringe or peristaltic pumps. Besides size and integration, an accurate flow rate, wide range of flow rate and low controlled errors are goals for all pumps in general.[79]

A standard approach in microfluidic pumping is the use of syringe or peristaltic pumps because of their preferred characteristics- stability and wide flow rate range.[80, 81] Nevertheless, the miniaturization and integration of a microfluidic device is difficult when it is bound to a bulky pump, especially, when the device needs more than one pump.[79] This thesis addresses the problems of a (1) bulky and (2) expensive periphery associated with integrated micropumps by (1) reducing the footprint with integrated solenoid valves and (2) lower material price.

Die approbierte gedruckte Originalversion dieser Diplomarbeit ist an der TU Wien Bibliothek verfügbar
The approved original version of this thesis is available in print at TU Wien Bibliothek.
TU Bibliothek Your knowledge hub WIEN

1.5 Aim of the thesis

The aim of this thesis was to develop a mechanobiological organ-on-a-chip platform to mechanically actuate organ-on-a-chip systems. This platform will have an integrated a solenoid valve system with on board control software and the option of a small vacuum.

This platform will be of small footprint, low-cost solution, with eight valves included in the housing. The approach to build the mechanobiological platform is to use commercially available components, to save time and money and custom make the remaining parts. A user interface is integrated to this platform, to ensure easy handling and control.

The platform detailed here has applications beyond the field of mechanobiology, as it is compact, adaptable and offers multiple digital and analogue interfaces for control. By providing multiple outlets for pneumatic compression, a vacuum system designed for degassing or stretching of cells and the means for a pneumatic (peristaltic) pump.

Since this platform is intended for tissue and organ-on-a-chip research, it was assessed on a wound healing chip. Physiological methods for wound generation are important, especially for wound healing research.

The functions and requirements for this platform are:

Functions:

- Constant or cycled pneumatic pressure
- Pneumatic pump
- Small footprint
- Small vacuum (i.e., degas- function)

Requirements:

- Pressure change over external parts
- Limited in size
- Low-cost

Die approbierte gedruckte Originalversion dieser Diplomarbeit ist an der TU Wien Bibliothek verfügbar
The approved original version of this thesis is available in print at TU Wien Bibliothek.
TU Bibliothek Your knowledge hub WIEN

2. Materials and Methods

The mechanobiology platform consists of a pneumatic and an electronic system. The valve status is controlled by a user interface (UI) with an LCD display and rotary encoder. After manufacturing custom parts via additive manufacturing and assembling the platform, the device performance was assessed on a biochip with dermal fibroblasts. A complete list of materials is provided in Chapter 2.8.

2.1 Pneumatic system design

The pneumatic schematic was developed in FluidSim® 5 Home Use and FluidDraw® P5 from Festo. Pressure supply line and solenoid valves as well as valves and biochip are connected with polyvinyl chloride PVC tubing. Barbed Polypropylene t-shaped tubing connectors connect the valve with a biochip. The solenoid manifold includes eight body ported, super compact, direct acting 2/3 port solenoid valves. The solenoid valves have a coil voltage of 12 volts of direct current VDC, a power consumption of 0.35 W with an operation noise level on 38 dB or less. The SMC valve has a width of 7 mm with a weight of 5 g per single unit valve. It has a nozzle size of 0.5 mm and a maximum vacuum pressure of -88 kPa. The box style vacuum ejector comes with an built-in silencer [82]. The solenoids used for this thesis are compact direct operated 3 port solenoid valves mounted on a base of eight. It is a fast-switching 3/2 - way valve with spring return. The solenoids pressure should not exceed 0.6 MPa. The pressure control is directly mounted on the main pressure line over an operating valve.

2.2 Electronic subsystem and evaluation

The design and simulation process for the electronic subsystem was performed with EAGLE (Autodesk™) and LT Spice (Analog Devices™, Inc.) respectively. Different driver circuits were evaluated by comparing characteristics from data sheets. A

Die approbierte gedruckte Originalversion dieser Diplomarbeit ist an der TU Wien Bibliothek verfügbar
The approved original version of this thesis is available in print at TU Wien Bibliothek.
TU Bibliothek Your knowledge hub WIEN

test set-up was built to verify performance and function. The 6225P-model high precision digital laboratory power supply from PeakTech ® powers the circuit load (solenoid valves) during the performance tests. Jumper wires and a breadboard connected the driver circuit with the load. The circuits status was observed with a digital 117 Multimeter from Fluke.

A commercially available prototyping board, an Arduino Uno Rev3, was used for the mechanobiological platform. The Arduino Uno Rev3 comes attached with an programmable AT-mega328P microcontroller and 14 digital Input/Output (I/O) pins. The parts for the user interface (i2c module and rotary encoder) were connected according to the pin diagram of the microcontroller board. The full pin diagram is shown in Figure 2.1. The driver circuit and header were soldered on a modular circuit board that was subsequently stacked upon the Arduino.

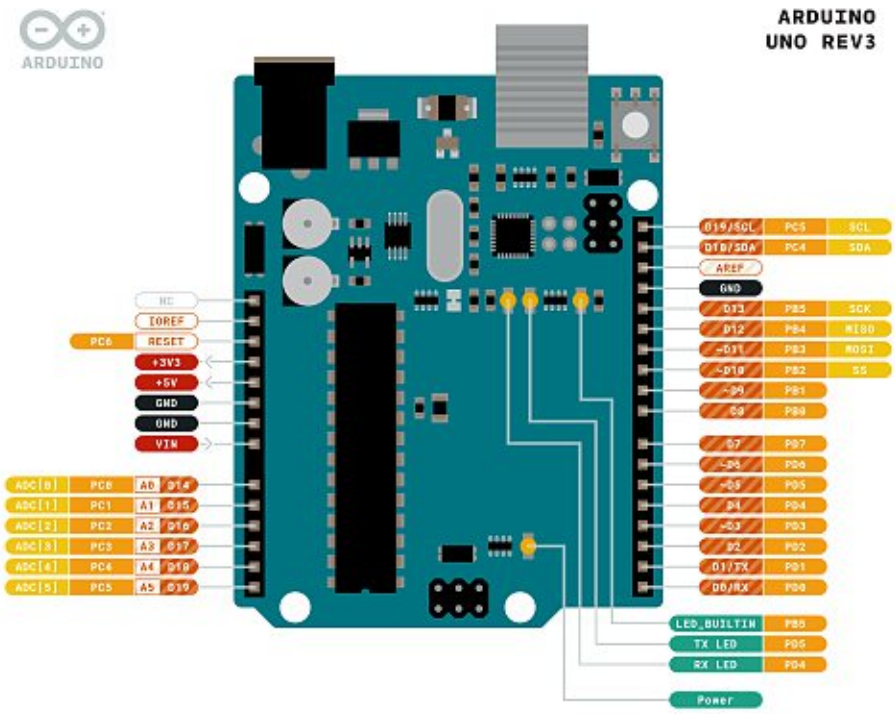

Figure 2.1: Pin Diagram Arduino Uno Rev3
The pins are color-coded: black = ground, red = power, grey = internal pin, orange striped = digital pin, white striped = analog pin, orange = microcontroller port, yellow = default, blue = LED and white = other. Pin Diagram provided by Arduino [83].

Die approbierte gedruckte Originalversion dieser Diplomarbeit ist an der TU Wien Bibliothek verfügbar
The approved original version of this thesis is available in print at TU Wien Bibliothek.
TU WIEN Bibliothek Your knowledge hub

A common ground was established by connecting the valves ground and the ground of the Arduino. The positive wire of the 12V power supply was connected to the common ground (pin 10) of the ULN2803a and the solenoid valves via header on the modular circuit board. Pins 1-8 of the ULN2803a were connected to the output pins (2-9) of the Arduino. The valves were connected to the remaining pins (11-18) of the ULN2803a. The Arduino was separately powered by a USB B to USB A cable connected to the PC. It provides 5V and up to 2A as power source. A Fluke 568 Contact and Infrared Temp Gun was used to estimate the dissipated heat. The temperature was measured on a full running circuit every minute for 20 minutes and every 10 minutes for the following 5 hours.

2.3 Additive manufacturing

The housing was designed with the AutoCAD® (Autodesk®) Software and manufactured with a fused deposition modelling FDM printer. The 3D printer used are an Original Prusa i3 MK3S printer with a magnetic polyetherimide PEI spring steel print sheet and an Original Prusa i3 MK2s. The layer height was set to 0.2 mm with a 0.4 mm hardened steel printing nozzle from E3D (E3D-Online). Bottom and top layers are printed solid with 100% infill. The overall fill density gradually decreased to the set value of 5%. The parts are printed with perimeters of three. The printing speed was set to 60 mm/s for perimeters, 80 mm/s for infill and 130 mm/s for non-printing movements. The filament material was Polyactic Acid (PLA) with a diameter of 1.75 mm. The first layer is extruded with a nozzle temperature of 220 ° C, with 210° C for every other layer. The heat bed is set do 60° C. After printing, the support material was removed with needle-nose pliers and an exacto knife and the parts rinsed with isopopyl alcohol.

2.4 Programming

The ATmega328P microcontroller (mounted on the Arduino Uno R3) was programmed using the Arduino® Integrated Development Environment (IDE) version 1.8.13 which was downloaded from the official Arduino website and installed on Windows 10. To program the microcontroller, the Arduino was connected to the PC via USB B to USB A cable and IDE configurations were made. The IDE was configured by selecting the assigned COM port number and the board. The program was written in C/C++. The code was verified and compiled by the IDE prior to uploading.

The user interface (UI) consists of a 16x2 liquid crystal display LCD connected to an i2c module (AZ-Delivery) and a rotary encoder. The i2c module as well as the

Die approbierte gedruckte Originalversion dieser Diplomarbeit ist an der TU Wien Bibliothek verfügbar
The approved original version of this thesis is available in print at TU Wien Bibliothek.
TU Bibliothek Your knowledge hub WIEN

rotary encoder were connected to the microcontroller board. A button cap was printed to fit the KY-040 rotary encoder (Joy-it). A graphical UI was designed and programmed with Processing (version 3.5.4) in JavaScript. Libraries were added for the serial communication and the UI: Wire.h, LiquidCrystal_I2C.h, processing.serial and controlP5 respectively. The communication protocol for the master/slave bus is adapted from the library documentation.

2.5 Experimental set-up

The previously published wound healing chip design [37] used for the experiment includes three PDMS layers between two microscope slides. The top layer consists of the pneumatic structures while the middle and bottom layers house the microfluidic channels. A sketch of each layer is shown in Figure 2.2. For the PDMS reservoir strips, silicon curing agent and silicon elastomer base were mixed in a ratio of 1:10. The liquid PDMS was degassed using a desiccator for about 20 min before filling the molds. The filled molds were then covered with foil and placed in a 70°C oven until cured. Once cured, the reservoir strips were removed from the mold using 70% ethanol and cut to size. The reservoirs were punched into the PDMS strip using a 6mm biopsy puncher.

The 250 µm thick PDMS foil (MVQ Silicones GmbH, Germany) was cut into the designed shape within a 76 mm x 26 mm rectangle using xurography. The access holes in the covering microscope slide were drilled in water using a drill press machine and a custom 3D printed drilling template. The diameter of the drill was 1 mm. The glass slides were cleaned in an ultrasound bath. First in a 2% Hellmanex III solution, then isopropanol and lastly deionized water. The cleaned slides were further air dried and kept in a 80°C oven to dry off completely before bonding. The bonding of the layers, as well as the PDMS reservoir strips was performed with a superficial plasma treatment for 2 min. The individual layers were first plasma treated, then aligned, placed and pressed together. The assembled biochip was then placed in a 80°C oven over night. Only two layers were handled at a time. Finally, 1 cm long polymer tubes were glued to the ports on the top glass using epoxy glue. To cure the glue, the biochips were placed in a 70°C oven for at least 2 hours.

The microchannel was rinsed with 70% ethanol and DPBS, prior to surface coating. For surface coating, the microchannels were filled with a 0.09% collagen I solution and incubated for 2 h at 37°C. The coating solution was then removed from the microchannels. A cell suspension with a cell concentration of 600 cells per mL was inserted into the microchannels and reservoirs until the surface tension reached its peak. The biochips were then incubated 7°C, 5% CO_2 until sufficient confluency was reached. To counteract the medium evaporation, a flask bottle cap was filled with medium and placed next to the biochips while incubated.

Die approbierte gedruckte Originalversion dieser Diplomarbeit ist an der TU Wien Bibliothek verfügbar
The approved original version of this thesis is available in print at TU Wien Bibliothek.
TU WIEN Bibliothek Your knowledge hub

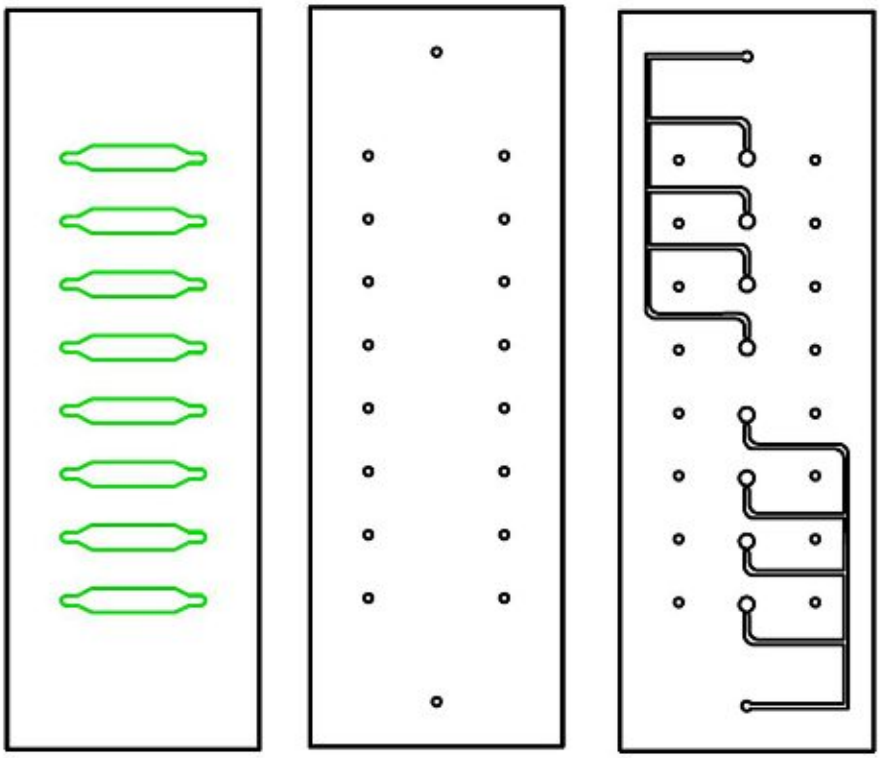

Figure 2.2: Chipdesign
Sketch of each PDMS layer of the chip from bottom layer (left) to top layer (right). Figure adapted from [37].

The biochip was connected to the platform with PVC tubes and barbed t-shaped tubing connectors. The platform itself was connected to the main pressure line, with the pressure set at 4.5 bar. The opening and closing of the valves was controlled over the UI. The time, on which pressure was applied, was less than two seconds. At each step, images were taken using a microscope. Further analysis was performed with a fluorescent microscope.

2.6 Cell culture

The primary Human Dermal Fibroblasts (HDF) used for this experiment originated from human foreskin (pooled). The frozen cryotube containing HDFs was taken from liquid nitrogen and placed in a 37°C water bath until 80 % thawed. The cell suspension was then transferred into a 15 ml falcon and 8 ml fibroblast growth medium was added. The medium consisted of Dulbecco's Modified Eagle Medium (DMEM) high glucose, 10% Fetal Bovine Serum (FCS) and 1% Antibiotics. After

Die approbierte gedruckte Originalversion dieser Diplomarbeit ist an der TU Wien Bibliothek verfügbar
The approved original version of this thesis is available in print at TU Wien Bibliothek.
TU Bibliothek Your knowledge hub WIEN

centrifugation, the supernatant was removed, and the remaining cell pellet resuspended in 1 ml medium. It was then transferred into a T75 flask with additional 8 ml medium and incubated at 37°C, 5% CO_2 until 90% confluency was reached. With the confluency at the desired level, the medium from the T75 flask was aspirated. The cells were then washed twice with 5 ml Dulbecco's Phosphate-Buffered Saline (DPBS) and treated with 3 ml of a trypsin solution and incubated for 5 min or until detached (examined using a microscope). The reaction was stopped with 5 ml of fresh medium added to the trypsin-cell-suspension. The cell suspension was transferred into a falcon tube and cells were counted.

For cell counting, 10 μl of the cell suspension were mixed with 10 μl Trypan Blue and centrifuged. The Trypan Blue-cell-suspension was then placed in a Neubauer cell counting chamber and cells were counted using a microscope. Cell count was then determined with the following equation:

$$cells/ml = \frac{cells_{counted}}{area_{counted} * depth_{chamber}} * dilution * 1000 \tag{2.1}$$

The supernatant was discarded, the remaining cell pellet again resuspended in culture medium and centrifuged. An aliquot with the appropriate cell number was added to a new flask with culture medium and again cultivated at 37°C, 5% CO_2.

2.7 Imaging

During pneumatic wounding, the biochip was placed under a microscope (Olympus IX81) for monitoring and imaging. For imaging the channel and/or the pressurized area, 4x and 10x magnification objectives were selected, respectively. After wounding, the chips were placed in a life cell microscope (Cell Vivo) for fluorescent imaging. DAPI, FITC and/or TRITC channels were selected and brightness was adjusted to acquire the image.

Die approbierte gedruckte Originalversion dieser Diplomarbeit ist an der TU Wien Bibliothek verfügbar
The approved original version of this thesis is available in print at TU Wien Bibliothek.
TU Bibliothek Your knowledge hub WIEN

2.8 List of materials

Table 2.1: List of Materials

Materials	Manufacturer
Antibiotics	Sigma Aldrich
Arduino Uno Rev3	Arduino
Biopsy puncher	Stiefel
Cutting Plotter	Roland
Cell culture flasks	Greiner BioOne
Cell tracker	Thermo Fisher Scientific
CellVivo Life cell microscope	Olympus Life Sciences
Centrifuge	Eppendorf
Collagen I	Sigma - Life Science
DC/DC Converter 12V-5V	RS Pro
DMEM high glucose	AppliChem
DPBS	Sigma Life Science
Drill Press	PROXXON
EIC-J-L Jumper set	TRU Components
Epoxy glue	Henkel
Ethanol 70%	VWR Chemicals
Extrusion printer	Prusa
Falcon tube	Falcon
FCS	Sigma - Life Science
Female header straight RM 2.45 1x8 pol	W+P

Die approbierte gedruckte Originalversion dieser Diplomarbeit ist an der TU Wien Bibliothek verfügbar
The approved original version of this thesis is available in print at TU Wien Bibliothek.
TU Bibliothek Your knowledge hub WIEN

Table 2.1 continued from previous page

Materials	Manufacturer
Fluorescein	Sigma Aldrich
Hellmanex III	Hellma Analytics
HDF	CELLNTEC
Incubator	Eppendorf
IC-Fassung 18-polig	Conrad
IC ULN2803A DIL 18	STMicroelectronics
i2c adapter	MH
Isopropanol	VWR Chemicals
Laminar-flow hood	Thermo Electron
LCD	Joy-it
Microscope	Olympus Life Sciences
Microscope glass slide	VWR
Mini Protoshield board shield	IDUINO
Pasteur pipette	Greiner Bio-One
PDMS foil	MVQ Silicones
Petri dish	Greiner Bio-One
Plug-in Power Supply	Dehner Elektronik GmbH
Pipette tips	ep T.I.P.S.
Pipettor	SARSTEDT
Polymer tubes	TYGON
Prusament PLA Gentlemen's Grey	Prusa
Prusament PLA Vanilla White	Prusa

Die approbierte gedruckte Originalversion dieser Diplomarbeit ist an der TU Wien Bibliothek verfügbar
The approved original version of this thesis is available in print at TU Wien Bibliothek.
TU Bibliothek Your knowledge hub WIEN

Table 2.1 continued from previous page

Materials	Manufacturer
Rotary encoder	Joy-it
Silicon curing agent	SYLGARD
Silicon elastomer base	SYLGARD
Solder	RS Pro
Soldering station	Weller
Trypsin/EDTA	Sigma Aldrich
Water bath	Grant Instruments
10 μH TC-HBCC-100K-00203 Induction	TRU Components
22 μF/10V Capacitor	Panasonic
10 μF Capacitor	Yageo Corporation

Die approbierte gedruckte Originalversion dieser Diplomarbeit ist an der TU Wien Bibliothek verfügbar
The approved original version of this thesis is available in print at TU Wien Bibliothek.
TU Bibliothek Your knowledge hub WIEN

3. Results

The overall goal of this thesis was to provide a simplified, user-friendly, low-cost solution to control solenoid valves. The system was designed with a focus on modularity and versatility. As such, various hardware configurations are supported. The components listed in the bill of materials 3.3 reflect the current configuration. The mechanobiological organ-on-a-chip platform consists of three subsystems: (1) a pneumatic control system connected to an (2) electronic driver circuit and (3) a user interface and control software. Each subsystem is described in the subsequent sections.

3.1 System periphery to facilitate biomedical implementation

An external pneumatic infrastructure is necessary for operating microfluidic systems with on-chip valves. The pneumatic subsystem is designed to connect the solenoid valves with a compressed air pressure source. The electro-pneumatic system design is shown in Figure 3.1. The system is designed to control a manifold of eight solenoid valves with pressure from the supply elements and the electronic status control from the electronics. The compressed air pressure is supplied by a main pressure line, connected to a pressure gauge. A manifold of eight body-ported solenoid valves is connected to the pressure supply. An inline vacuum ejector is connected to one valve to facilitate additional and advanced applications. Leaving seven valves for individual control. A three-valve pneumatic peristaltic pump is implemented. For the pneumatic peristaltic pump, a sequential opening and closing sequence is programmed. This paired with a microfluidic device with three pneumatic membrane actuators (microvalves) generates a squeezing motion of liquids. Thereby inducing the liquid flow in the fluidic layer on the microfluidic device. Each valve can be connected via a barbed connector and PVC tubes. The pneumatic is controlled by the electronic subsystem. This allows for precise control over the valve status. The solenoid valves and the electronic subsystem is integrated in a custom housing.

Die approbierte gedruckte Originalversion dieser Diplomarbeit ist an der TU Wien Bibliothek verfügbar
The approved original version of this thesis is available in print at TU Wien Bibliothek.
TU Bibliothek Your knowledge hub WIEN

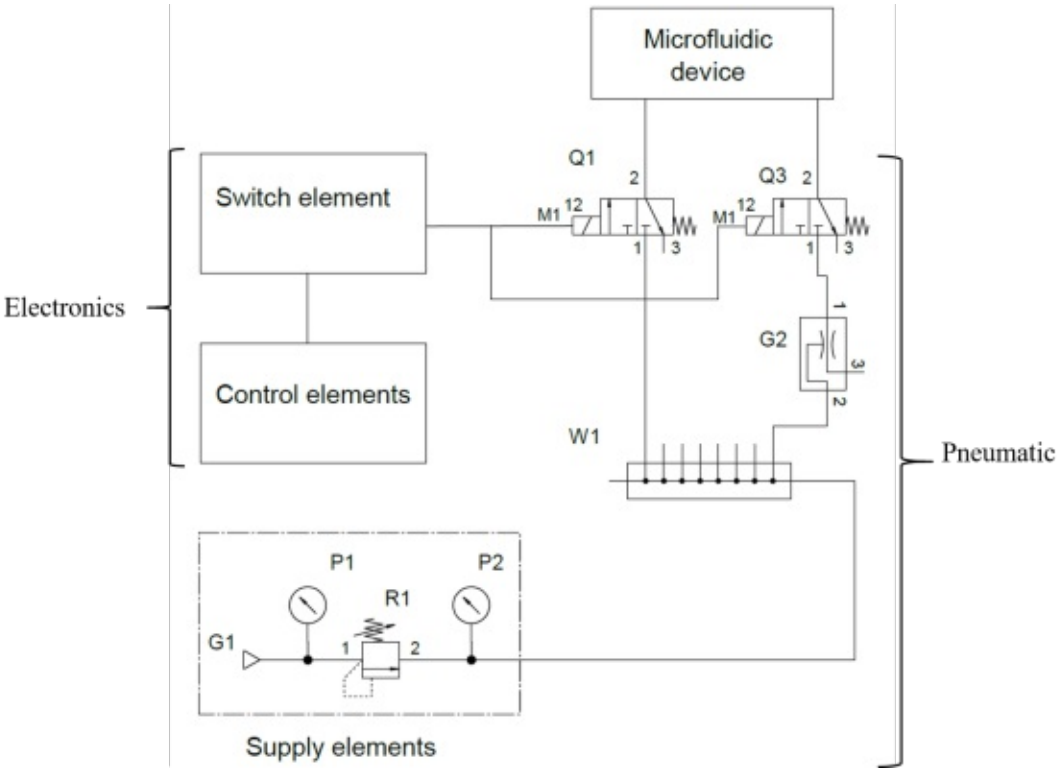

Figure 3.1: Electro-pneumatic System Design
Electro-pneumatic schematic with two valves (Q1, Q3) connected to a manifold (W1). Valve Q3 is further connected to a vacuum ejector element (G2) before being plugged to a microfluidic device. Control of the pressure with pressure gauge (P2) on a pressure supply element (e.g main pressure line). The valves are directly connected to the electronics.

3.1.1 Housing optimization

The individually designed housing optimally supports the mechanobiology platform by being modular and easy to assemble. Integrating the solenoid valves and the electronic subsystem into one housing allows for a compact platform which occupies little space on the benchtop. The housing is three-parted, with the bottom box including the electronics, the middle part holding the valves and the top part for the LCD display and rotary encoder button. This allows easy access to the different parts of the platform as well as a reduced manufacturing time. The housing is custom made and manufactured by fused deposition modelling. This has the advantage of a cost-effective fast manufacturing of the prototype and offers a wide range of printing

Die approbierte gedruckte Originalversion dieser Diplomarbeit ist an der TU Wien Bibliothek verfügbar
The approved original version of this thesis is available in print at TU Wien Bibliothek.
TU Bibliothek Your knowledge hub WIEN

material. It also allows for a less restricted, more complex design than traditional manufacturing processes. By using choosing this manufacturing method, unique features could be implemented to the platform's enclosure.

Fastening features

A circuit board must be kept in place to keep it and the components attached to it in the correct position. Therefore, a custom mounting system was designed which is integrated into the bottom part of the enclosure. A three-millimetre-deep notch allows for the Arduino to snap into place. This prevents unwanted movement of the electronic setup without the need of screwing the Arduino to the bottom. Figure 3.2 shows a top view and a side-cut of the notch. The bottom part includes two port openings on the left side. These openings allow for an easy connection of the power cables to the Arduino. The size of these openings fits the size of the mounted ports on the Arduino Uno Rev3.

The solenoid valve manifold is mounted on top of the bottom part. Therefore, a 25 mm wide cover was added to the bottom part. The valve manifold can be placed onto the 45° overhang. Due to a 1.5 mm x 1 mm offset, the manifold is prevented from falling off the bottom part. Alternatively, it can be screwed into place to afford further hold.

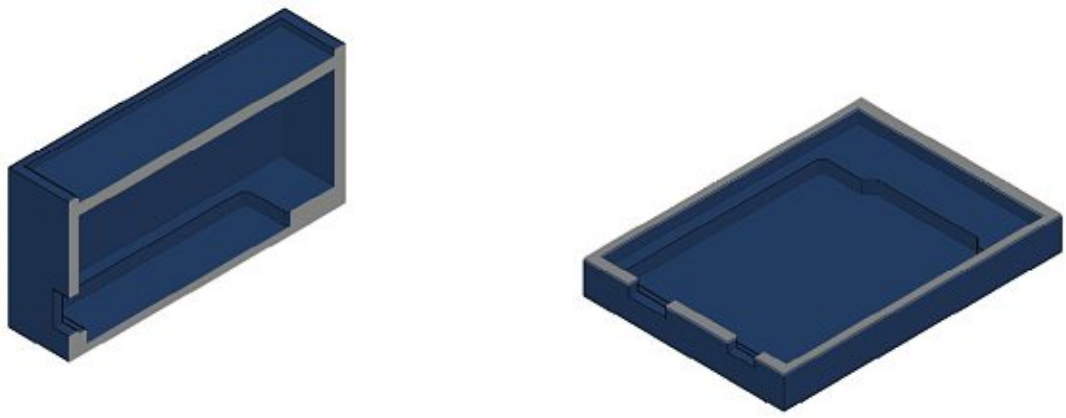

(a) Bottom detail - side view (b) Arduino snap notch - top view

Figure 3.2: Bottom Part Details
Snap detail in bottom part. Holds Arduino in place without any screws. Figure (a) shows the side-cut of the 3 mm deep notch as well as the 1 mm offset on the cover of the bottom part. Figure (b) is a top view of the bottom part, cut at 1 cm. It visualizes the complete notch as well as the connection ports.

Die approbierte gedruckte Originalversion dieser Diplomarbeit ist an der TU Wien Bibliothek verfügbar
The approved original version of this thesis is available in print at TU Wien Bibliothek.
TU Bibliothek Your knowledge hub WIEN

A middle part was added to connect the bottom and the top part. It provides the necessary distance to allow an easy and tension free connection of the electronics (valves and UI elements) to the Arduino. Adding an overhang and flanks to the middle part further secures the solenoid manifold on the bottom part (see Figure 3.3).

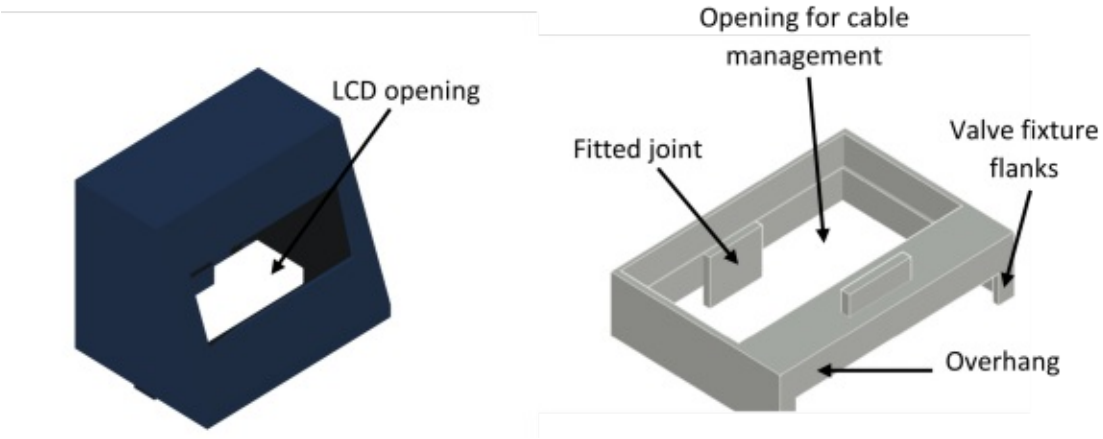

Figure 3.3: Middle and Top Part Details
Middle and top part of the platform housing. The two parts are connected with fitted joints on both, the top and middle part. Because the middle part is placed on the bottom part, it has also fitted joints on the bottom side. The topside is designed in an angle to facilitate LCD visibility. A small opening hole is on the right side for the rotary encoder knob. The front side of the middle part has an opening which fits the valve manifold while they are placed on the bottom part, thus holding it in place.

A number of fitted joints connect the parts. The middle part connects to the bottom part with a single joint placed on the middle part. While the top part is secured with four joints in total. Three on the top part, one on the middle part. The multiple snap fits assist with alignment of the parts and transfer the shear load across the part. A tolerance of 0.45 mm was considered during the design phase of the joints, to ensure perfect fit. The tolerance matches the printer's tolerance. The middle and top part were printed vertically (z-direction from the printing bed) to guarantee stability. This is necessary due to the anisotropic nature of 3D printed parts.

The top part encases the LCD and holds the button. Top part is designed as a right trapezium prism with an 70° angle. The angle allows for a better visibility of the LCD. The wall thickness for this part is increased to adjust for the weight of the LCD. Figure 3.4 shows the top and middle part connected by fitted joints on either part.

Die approbierte gedruckte Originalversion dieser Diplomarbeit ist an der TU Wien Bibliothek verfügbar
The approved original version of this thesis is available in print at TU Wien Bibliothek.
TU Bibliothek Your knowledge hub WIEN

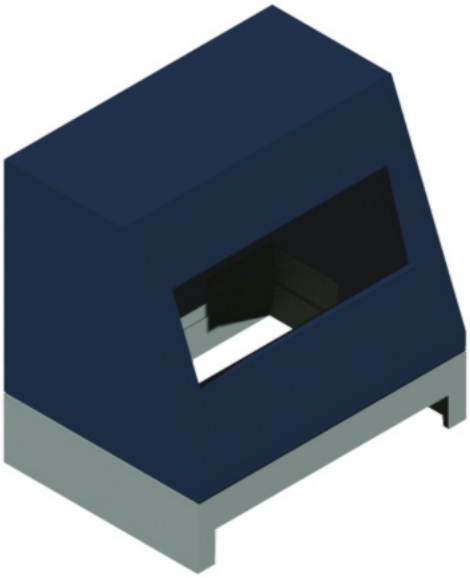

Figure 3.4: Middle and Top Part of the Platform
The top part is designed as a right trapezium prism with an 70° angle which allows for better visibility of the LCD. The two parts are connected by fitted joints on either part.

Die approbierte gedruckte Origi
The approved original version o
TU Bibliothek
Your knowledge hub
WIEN

Assembled mechanobiological platform

Figure 3.5 shows the mechanobiological platform as used in our laboratory, connected to a microfluidic biochip, the main air pressure line and a power supply. In this case a 12 V plug-in power supply. The connection between the platform and the microfluidic biochip is established through barbed connectors and PVC tubes. Two valves are connected to the biochip, as it has two pneumatic lines (see Figure 2.2. This setup is used for observing the effects of compression on dermal fibroblasts.

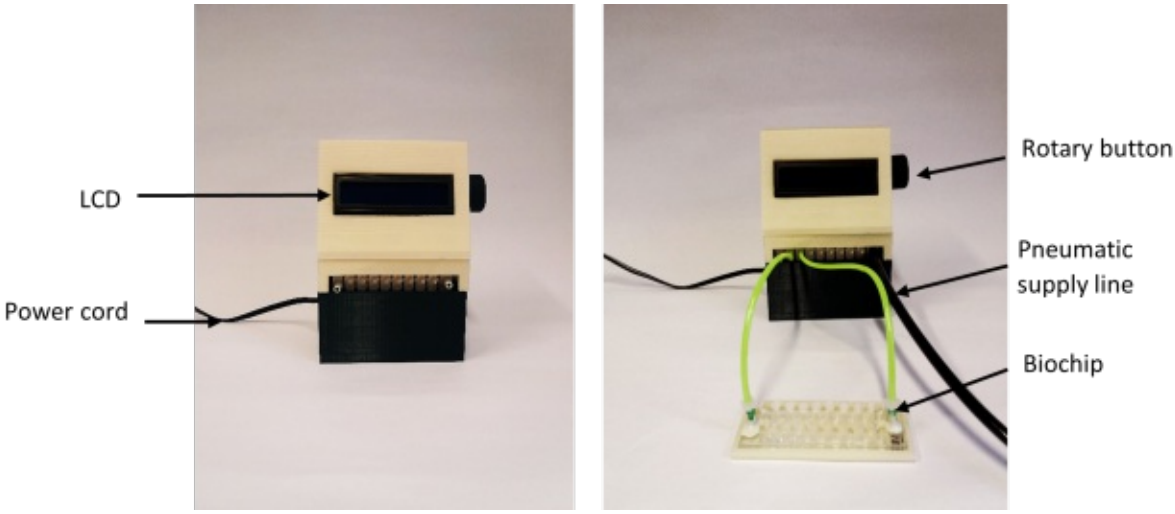

Figure 3.5: Assembled mechanobiological Organ-on-a-Chip platform
Assembled mechanobiological Organ-on-a-Chip platform. The platform includes three custom made parts - bottom, middle and top part. The bottom encloses the electronics while the solenoids are placed on top and are further enclosed by the middle part. The middle part allows additional room for wire connections, therefore preventing tension on the cables. The top part encases an 16x2 LCD with an i2C adapter module attached and a rotary encoder. A 3D printed knob is placed on the rotary encoder (right side).

Die approbierte gedruckte Originalversion dieser Diplomarbeit ist an der TU Wien Bibliothek verfügbar
The approved original version of this thesis is available in print at TU Wien Bibliothek.
TU Bibliothek Your knowledge hub WIEN

3.1.2 Microcontroller-based electronic system design

The electronic system includes the solenoid driver, the power supply as well as the electronics required for the UI. The driver method was chosen based on eight requirements as discussed in section. The resulting driver method is then further discussed. The application circuit is presented in chapter 3.1.2. A platform version has been designed that allows the connection of 40 valves.

Comparison of driver possibilities

The different methods of driving the load were evaluated based on the following criteria: life span, switching time, handling of loads, resistance to shock and vibration, size, prize, heat generation and efficiency. The different prospects were either tested with the test setup, see Figure 3.6 or by consulting the according datasheet. The tested devices can be grouped into relay and transistor-based switching methods. Mechanical and solid state relays were compared to Insulated-gate Bipolar Transistor (IGBT), Metal Oxide Semiconductor Field Effect Transistor (MOSFET) and Bipolar Junction Transistor (BJT). The result of this evaluation is listed in table 3.1.

Although both relays offer a complete separation of the circuitry, they are fairly slow and bigger in size, compared to transistor-based solutions. While they can handle high loads, the heat generation of the relay exceeds the heat dissipated by IGBTs and BJTs. IGBTs offer a slower switching time in a bigger body, compared to a BJT driver. MOSFETs on the other hand do not only offer a fast-switching time for high loads but are also very efficient. The drawbacks for this driver solution are the heat generation and the lack of small integrated driver solutions. Although a BJT is less efficient, the advantages of already available integrated driver circuits (Darlington pairs with flyback diodes) at low costs outweigh this drawback. Thus, a multi-transistor configuration - Darlington pair - is used for the platform.

Current amplification factor

Transistors are used to amplify a current of an input signal. To define the current amplification factor, the ratio of change in collector current to the corresponding change in base current is calculated. The amplification factor is called beta value. The beta value of a single bipolar junction transistor is typically between 20 and 200 for most general-purpose transistors. This current amplification of a single transistor is too low to directly drive the load. Therefore, a Darlington pair is used to increase the current gain.

Die approbierte gedruckte Originalversion dieser Diplomarbeit ist an der TU Wien Bibliothek verfügbar
The approved original version of this thesis is available in print at TU Wien Bibliothek.
TU Bibliothek Your knowledge hub WIEN

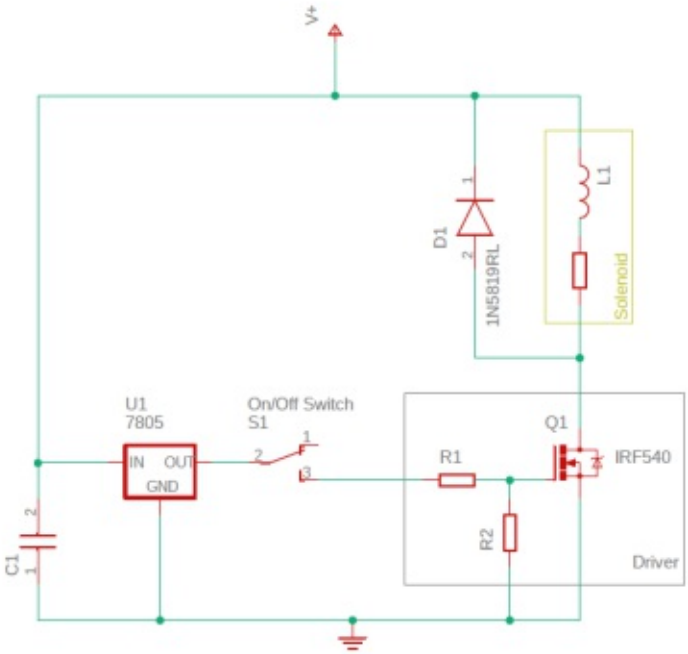

Figure 3.6: Equivalent circuit of a solenoid valve
The load of this circuit is the solenoid valve and is represented as an inductor in series with a resistor. A flyback diode is added parallel to the load to prevent voltage spikes across the inductive load once the supply current is interrupted. A bypass capacitor is parallel to the 12V power supply. A voltage regulator is part of the circuit to reduce the supply voltage to 5V and is connected to a switch. The switch enables easy control over the solenoid status (on/off). The driver circuit is changed to the testing needs.

Table 3.1: Driver comparison

	Solid State Relay	**Mechanical Relay**	**IGBTs**	**MOSFET**	**BJT**
Life span	low	low	high	high	high
Switching time	100µs (medium)	15ms (slow)	medium	fast	100ns (fast)
Handling of loads	high loads	high A/V loads	high A/V loads	high A/V loads	low loads
Shock/ vibration resistance	medium	medium	high	high	high
Size	big	big	medium	small	small
Prize	high	medium	low	high	low
Heat generation	high	high	low	high	low
Efficiency	high	low	n/A	high	medium

Die approbierte gedruckte Originalversion dieser Diplomarbeit ist an der TU Wien Bibliothek verfügbar
The approved original version of this thesis is available in print at TU Wien Bibliothek.
TU WIEN Bibliothek Your knowledge hub

This transistor configuration consists of two bipolar transistors connected in such a way that the current amplified by the first transistor is further amplified by the second transistor to provide a higher current gain. The lowest base current to sufficiently push the transistor into saturation is 3.6 mA, given a beta - value of 7000 for this application.

Transistor driver

Each channel of the ULN2803a consists of NPN transistors in a Darlington configuration. The resulting beta allows a high output current with a very low input current. Thus, enable an operation with general purpose input/output GPIO voltages. The input/output voltage is converted to base current through the 2.7 kOhm resistor connected between the input and base of the Darlington transistor [84].

The Darlington transistor array consists of eight NPN Darlington pairs. The ULN2803a features additionally high-voltage outputs with common-cathode clamp diodes. This enables switching inductive loads. The logic diagram of the ULN2803a is provided by the manufacturer (Texas Instruments) and is shown in Figure 3.7. When the voltage of the electrical load surpasses the supply voltage, one must connect the ground potential of both circuits. In case of driving inductive loads, like solenoid valves, the coil supply voltage must be connected to the COMMON pin (COM/Pin 10). Resulting in a short circuit of the IC caused by the self-induction of the internal flyback diodes.

Although the output current of the ULN2803a is limited to max. 500 mA, a load with higher switching current can be operated by connecting multiple outputs in parallel. In case of this special application and its components, it is not necessary to place additional flyback diodes near to the inductive load. But if the solenoid would be changed to larger ones in the future, it is something which should be considered.

Application circuit and issues

The solenoid driver circuit is soldered to a prototyping shield. The shield is then stacked on top of the Arduino Uno.The contact pins for the 3 V and 5 V must be removed on the prototyping shield to avoid damage to the microcontroller. Otherwise, the 12 V of the solenoid power supply would be connected to the 3 V power input on the microcontroller board since the existing PCB lines of the prototyping shield are used.

The Arduino Uno can be powered externally with up to 20 V either from the DC power jack (7-12 V) or the VIN pin on the board, as both are connected to the on-board regulator. This is important to note, when more than 3 V are connected.

Die approbierte gedruckte Originalversion dieser Diplomarbeit ist an der TU Wien Bibliothek verfügbar
The approved original version of this thesis is available in print at TU Wien Bibliothek.
TU Bibliothek Your knowledge hub WIEN

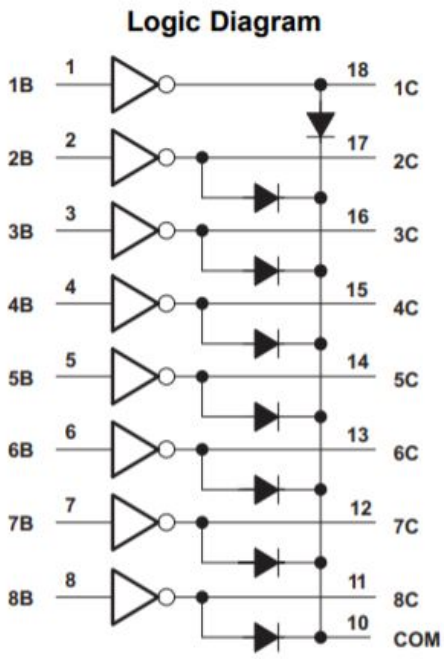

Figure 3.7: Logic Diagram of the ULN2803a
The ULN2803a device is a 50V, 500mA Darlington transistor array with common-cathode clamp diodes. This enables driving of inductive loads such as solenoid valves. The output pins may be connected in parallel for higher current amplification. Figure from [84].

If 12 V were to be connected to the 3 V input pin, it would bypass the voltage regulator, resulting in a damaged board. The 3V contact pin is removed to ensure that the 12 V supply from the solenoids does not pass to the Arduino Uno. The electronic system can be powered by a 12 V power cable or a battery pack with a capacity of 1500 mAh via the DC power jack.

The solenoid driver circuit is a Darlington transistor array with output diodes with soldered pin ports on each input and output. The ground is connected to the common ground of the microcontroller circuit and com to 12 V. Female Dupont connectors were crimped on the wires and then connected to the transistor array and the common ground. Female header pins were soldered to the shield for easy connections.

The temperature of the circuit was measured with a Fluke infrared heat gun on a fully operated circuit (all valves are activated/deactivated) every minute for 20 minutes and every 10 minutes for the following 5 hours. The temperature never exceeded 26°C during the measurement time. Based on this measurement, it can be determined, that there is no need to implement a fan or alternative heat sinks to this platform.

Die approbierte gedruckte Originalversion dieser Diplomarbeit ist an der TU Wien Bibliothek verfügbar
The approved original version of this thesis is available in print at TU Wien Bibliothek.
TU Bibliothek Your knowledge hub WIEN

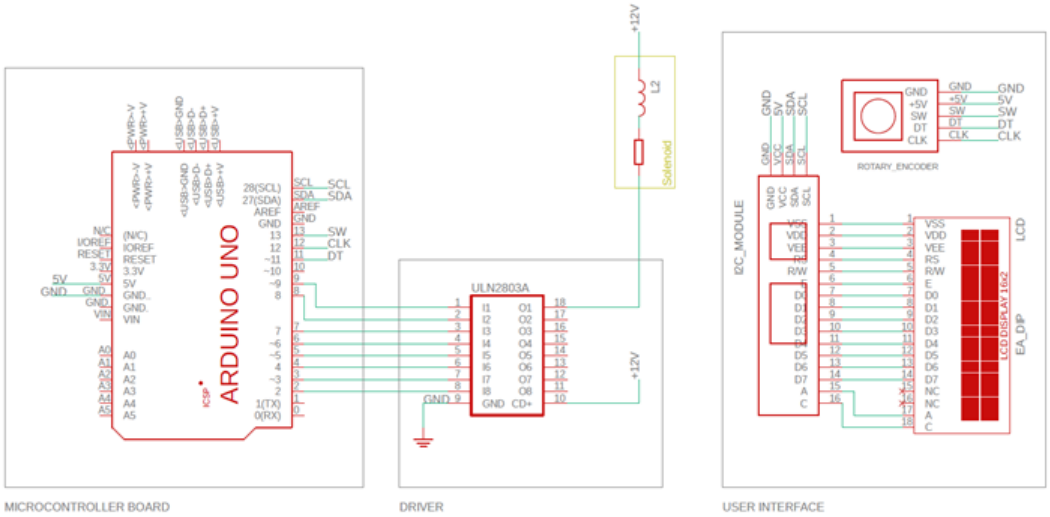

Figure 3.8: Solenoid circuit with UI
The circuit can be divided into four parts. The microcontroller board (Arduino Uno), the solenoid driver with the solenoid as a load and the user interface. The UI consists of an LCD connected to an I2C adapter module and a rotary encoder. The latter are connected to the microcontroller board. The driver is an ULN2803a Darlington transistor array connected to the inductive load -solenoid valve- and the microcontroller. The solenoid valves are represented as a resistor in series with a inductor.

3.1.2.1 Application upscaling

This platform in its current status is capable of controlling eight solenoid valves. The number of valves was specifically chosen to allow for a small platform footprint. Additionally, it is rarely necessary to actuate more than six pneumatic systems at once. Nonetheless, as those cases do exist, an upscaled version has been designed. It includes a custom Printed Circuit Board (PCB) and an Arduino Mega 2560. The solenoid driver system is the same for the upscaled version as for the regular 8-valve platform. The circuit and PCB layout are shown in Appendix A.1. The main idea of the upscaled version is that the Arduino Mega 2560 is stacked on the custom board to safe space and allow for heat dissipation, considering the greater area of the PCB. With this upscaled version, it is possible to control 40 individual valves at the same time.

Die approbierte gedruckte Originalversion dieser Diplomarbeit ist an der TU Wien Bibliothek verfügbar
The approved original version of this thesis is available in print at TU Wien Bibliothek.
TU Bibliothek Your knowledge hub WIEN

3.2 Software implementation

The associated software can be controlled over an LCD and rotary encoder. A direct form of programming of the microcontroller over the USB-B port is also possible. The control inputs do not necessarily correspond to the actual number of valves on the platform, only to the number of independent valves needed to perform the actuation. These connections are shown in chapter 3.1.2.

Figure 3.9: Graphical User Interface
A graphical user interface GUI for simple tasks. It is easy in use as it allows only to open/close either one or all valves.

The i2C communication protocol of the LCD and Arduino checks whether a start bit is received and ends when a stop bit is transferred. It then displays the transferred characters on the LCD display. The rotary encoder sketch detects (1) angular position displacement and (2) tactile button actuation. Because of the serial communication between the LCD and Arduino, the rotary encoder is read with interrupts. Using interrupts to read the encoder allows a quick reaction, as it disrupts the program flow instead of waiting for a communication to finish. This is especially practical when the wire.h library (serial communication) is used. Since the library has a busy wait period in it, the processor (16MHz) must wait until the 100kHz serial communication is completed before continuing with the program. Therefore, all transitions are received, and the menu handling feels precise. An alternative UI was programmed for simple tasks, such as opening and closing of either one or all

Die approbierte gedruckte Originalversion dieser Diplomarbeit ist an der TU Wien Bibliothek verfügbar
The approved original version of this thesis is available in print at TU Wien Bibliothek.
TU WIEN Bibliothek Your knowledge hub

valves. It is shown in Figure 3.9.

For debugging and advanced control options, a third way of controlling the platform was implemented. The user is able to precisely control the software functions by using a serial communication console, provided by the Arduino IDE. The user will be able to distinguish between two modes (pumping and compression) as well as set the running time for the mode of choice. The console input for pumping and compressing would be "1" and "2", respectively. By typing "t" (for time) and a number, the user can set the time/duration for the chosen mode. The distinctive algorithm for the platform is depicted in Figure 3.10. The user interface was tested with Windows 10.

Die approbierte gedruckte Originalversion dieser Diplomarbeit ist an der TU Wien Bibliothek verfügbar
The approved original version of this thesis is available in print at TU Wien Bibliothek.
TU Bibliothek Your knowledge hub WIEN

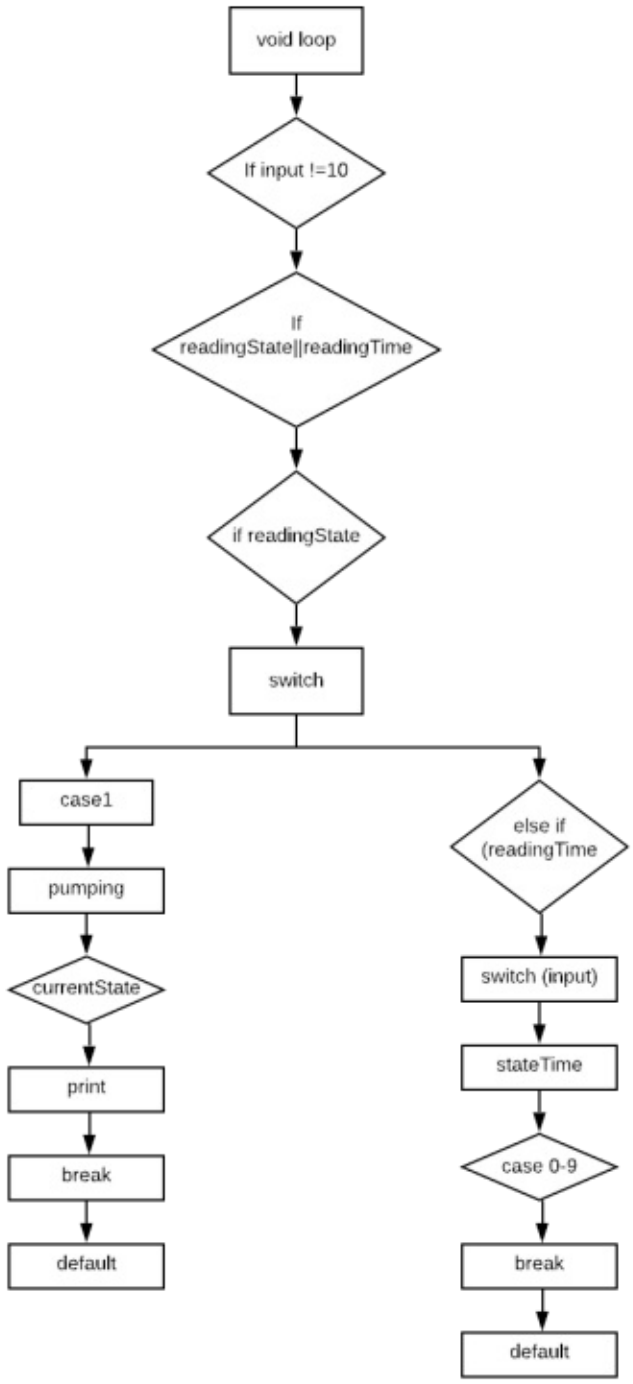

Figure 3.10: Program flow
Graphical visualization of the program flow. The void loop indicates a continuous loop. Firstly, it checks whether the user pressed the enter key by comparing the ASCII code for this input. If not, the program proceeds with the differentiation of the input - state or time. If the input was "t" the program waits for further input of the user to choose between pumping and compression and select its case accordingly. If a time was entered, it is converted to numeric and for each time it was pumped, a variable is incremented. When the entered time is equal to the variable, the program stops.

Die approbierte gedruckte Originalversion dieser Diplomarbeit ist an der TU Wien Bibliothek verfügbar
The approved original version of this thesis is available in print at TU Wien Bibliothek.
TU Bibliothek Your knowledge hub WIEN

3.3 Bill of materials

The aim of this thesis was to develop a mechanobiological organ-on-a-chip platform to lower the entry barrier for microfluidic and mechanobiological researchers. By reducing the material cost to less than 100 €, it is significantly cheaper to comparable devices where the price ranges from 500 € to over a thousand euro. [38, 60–62] The significant cost reduction is achieved by reducing the number of valves and choosing cheaper user interface hardware.

The following table is a global list of materials. It does not include the devices needed to manufacture the platform, in particular a 3D printer, soldering iron and solder. The full list of materials can be found in chapter 2.8.

3.4 Operation instructions

To operate the platform, it must be connected to either a pneumatic line or an external pump. When using a pneumatic pump, the pressure should be limited depending on the valve limits (see Datasheet). Said information can be found on the datasheet. The electronic system can be powered over a 12 V power cable or a battery pack with a capacity of 1500 mAh and can be connected via the ports on the bottom part. Rotating the button on the side of the top part will allow the user to scroll through the menu. To select a valve or program, the button must be pressed.

An alternative way to operate the platform is by using the Processing i3 user interface on a Laptop or PC which bypasses the user interface with the LCD display. For this manual operation mode, both, the Processing IDE and Arduino IDE must be installed. Then the firmware provided on Github. Once the Arduino IDE is open and a connection is established to the Arduino, the user may open and upload the firmware. The user then opens the GUI file in Processing. Once the run-button is pressed, the GUI window appears and the user is able to control the state of the valve by pressing the button on the screen.

Die approbierte gedruckte Originalversion dieser Diplomarbeit ist an der TU Wien Bibliothek verfügbar
The approved original version of this thesis is available in print at TU Wien Bibliothek.
TU Bibliothek Your knowledge hub WIEN

Table 3.2: Bill of Materials - Platform only

Component	No.	Cost/Unit	Total Cost	Supplier	EAN	Material Type
Arduino Uno Rev3	1	20	20	Arduino	8058333490090	Microcontroller board
Mini Protoshield board shield	1	6.33	6.33	IDUINO	4016139159751	Protoshield
Rotary encoder	1	3.99	3.99	Joy-it	COM-KY040RE	Rotary encoder
LCD	1	7.79	7.79	Joy-it	4250236815497	LCD display
i2c adapter	1	3.21	3.21	MH	9900002909992	Display interface
IC-Fassung 18-polig	1	0.25	0.25	Conrad	2050000074219	IC-socket
IC ULN2803A DIL18 STM	1	0.39	0.39	STMicroelectronics	2050000057328	Darlington transistor array
Female header straight RM 2.45 1x8 pol	2	0.65	1.3	W+P	2050001143747	Female header
DC/DC Converter 12V-5V	1	2.05	2.05	RS Pro	193-3976	DC/DC Converter
10µF Capacitor	1	0.05	0.05	Yageo Corporation	2050000119378	Capacitor
22µF/10V Capacitor	1	0.29	0.29	Panasonic	2050004354010	Capacitor
10µH TC-HBCC-100K-00203 Induction	1	0.35	0.35	TRU Components	2050004967326	Induction
EIC-J-L Jumper set	17	0.09	1.46	TRU Components	4016139223797	Cable
Plug-in Power Supply	1	9.99	9.99	Dehner Elektronik GmbH	4251125201124	Power Supply
S070M-6DC-32 valve, body ported, stacking, S070 solenoid valve, 3-port	1	34.81	34.81	SMC	S070M-6DC-32	Solenoid Valve
Prusament PLA Gentlemen's Grey	1	24.99	1.38	Prusa	PRM-PLA-GMG-1000	Printing Filament
Prusament PLA Vanilla White	1	24.99	1.78	Prusa	PRM-PLA-WHT-1000	Printing Filament
SUM			**95.42**			

Die approbierte gedruckte Originalversion dieser Diplomarbeit ist an der TU Wien Bibliothek verfügbar
The approved original version of this thesis is available in print at TU Wien Bibliothek.
TU Bibliothek Your knowledge hub WIEN

3.5 Validation and characterization of the platform

The mechanobiological platform performance was validated with a wound healing biochip. As the biochip consists of multiple Polydimethylsiloxane (PDMS) layers, including a pneumatic layer, a membrane deflection can be observed when pressurized air is led into the chip. The pressure applied was 4.5 bar due to preliminary data showing ideal membrane compression between 4 and 5 bar.[37].

The intention of this experiment was to mechanically induce circular cell-free areas in 2D cell-based models based on pneumatically actuated membranes. This experiment shows one of many potential application fields for this platform. The experimental set-up is shown in Figure 3.11. It includes the mechanobiological Organ-on-a-Chip platform and the manufactured wound healing chip connected with PVC tubes.

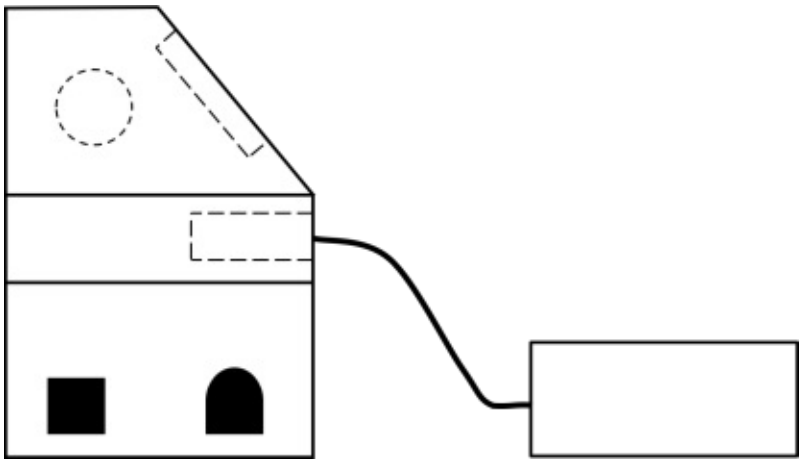

Figure 3.11: Experimental set-up
The experimental set-up includes the mechanobiological Organ-on-a-Chip platform connected to a wound healing chip. The platform pneumatically actuates membranes on the biochip thereby crating circular cell-free areas.

The wound healing chip was fabricated and tested for leakage prior to the experiment. The biochip is an assembly of five layers - two microscope glass slides, three PDMS. Figure 3.12c shows the fabricated biochip with medium filled microchannels. The wound healing chip consists of eight microchannels, each connected to a pneumatic layer. The microchannels can be perfused through inlets on the top glass independently on either side. The pneumatic layer is connected to ports on the surface glass and are used to connect the platform with the biochip.

Die approbierte gedruckte Originalversion dieser Diplomarbeit ist an der TU Wien Bibliothek verfügbar
The approved original version of this thesis is available in print at TU Wien Bibliothek.
TU Bibliothek Your knowledge hub WIEN

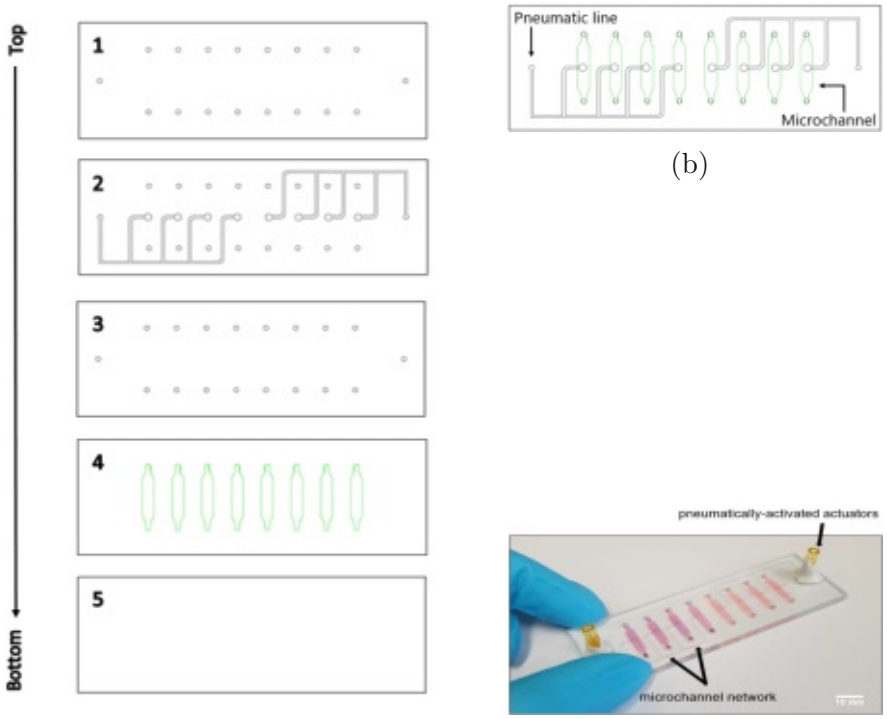

(a) (b) (c)

Figure 3.12: Wound healing biochip
Schematic illustration of the wound healing biochip without PDMS reservoirs. (a) The different layers are depicted with notation of their internal position (1-5). Layers 1 and 5 are microscope glass slides, whereas layers 2-4 are cutted PDMS foils. Layer 2 is referred to as 'pneumatic line' with layer 3 acting as membrane. Layer 4 is the microchannel network. Figure (b) shows the layers placed on top of each other while Figure (c) is the fabricated chip. The microfluidic chambers in Figure (c) were filled with colored water for visualisation. Figure (c) and chip design taken from Monfared et al. [37]

The pneumatic layer consists of lines connected to a round middle membrane (see Figure 3.12b), with the membrane positioned on top of the microchannel. When pressure is applied to this membrane it deflects, thus pressing on the microchannel.

3.5.1 Effect of compressive stress on dermal fibroblasts

When the membrane is deflected, it presses against the cell-seeded microchannel. This results in a circular cell-free area where the size depends on the applied pressure. The higher the pressure, the bigger the diameter of the cell-free area. With a pressure of 4.5 bar, the diameter is at its maximum with the given membrane ge-

Die approbierte gedruckte Originalversion dieser Diplomarbeit ist an der TU Wien Bibliothek verfügbar
The approved original version of this thesis is available in print at TU Wien Bibliothek.
TU Bibliothek Your knowledge hub WIEN

ometry [37]. The duration of the actuation was approximately one second. As this duration is more than sufficient for the membrane deflection and the resulting wound generation. The actuation was constantly observed with a microscope. A cell culture was established in the microchannels to demonstrate wounding on the biochip. An image of the microchannel freshly seeded with cells is shown in Figure 3.13a. The membrane deflection was tested on a biochip with water-filled microchannels. Figure 3.13b shows the deflected membrane pressing on the microchannel.

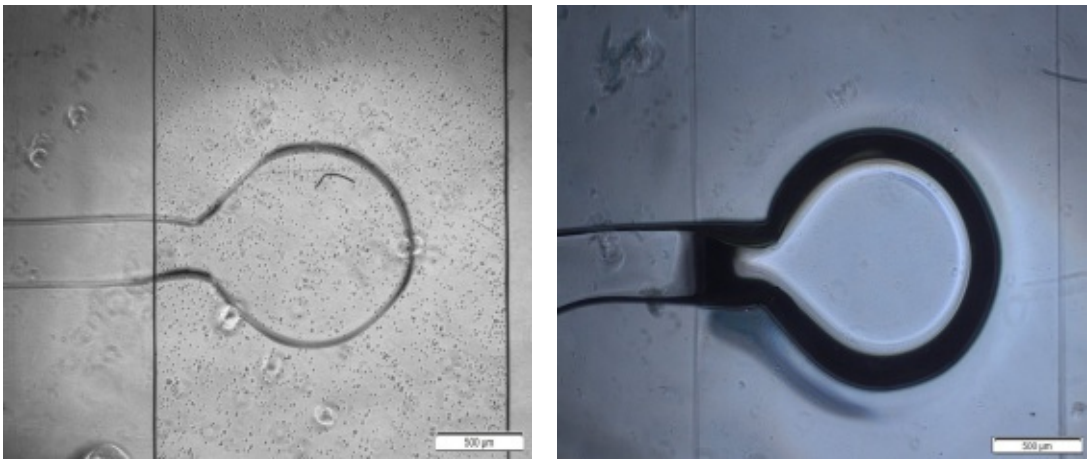

(a) Microchannel (b) Test with water

Figure 3.13: Close-up of the microchannel
Figure (a) shows the microchannel with the circular membrane in its middle after being seeded with HDF. The cells are rounded and not yet attached to the surface of the microchannel. Figure (b) shows the deflected membrane pressing against the underlying microchannel. The channel is in this case filled with water and a pressure of 4.5 bar was applied. Scale = 500µm.

Cell viability in and on the edges of the cell-free area were investigated by live-dead staining. Fluorescence imaging proved the premise of a cell-free area due to membrane deflection. A clear distinction between the treated area and the non-treated area is visible and can be seen in Figure 3.14a. Dead cells are spotted on the membrane and in the circular wounding area, while mostly living cells could be observed in the surrounding area (see Figure 3.14b). A close-up on the edges shows (Figure 3.14c), that only a few dead cells are present on the edges while the majority sticks to the membrane at the wounding.

Die approbierte gedruckte Originalversion dieser Diplomarbeit ist an der TU Wien Bibliothek verfügbar
The approved original version of this thesis is available in print at TU Wien Bibliothek.
TU Bibliothek Your knowledge hub WIEN

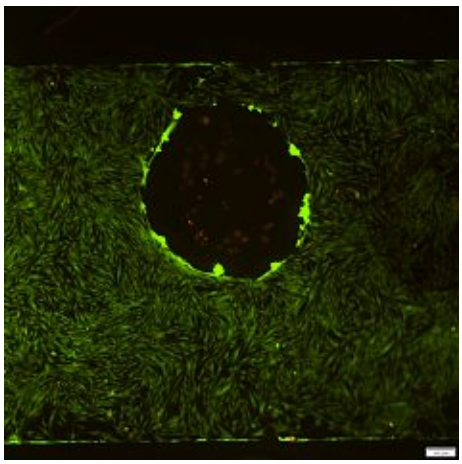

(a) Cell free area

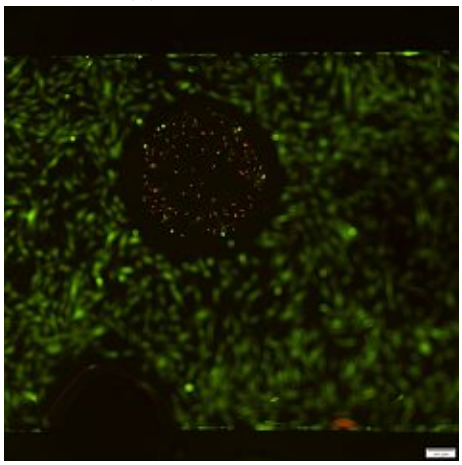

(b) Presence of dead cells

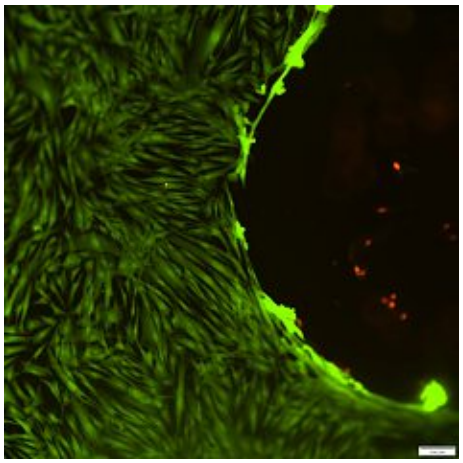

(c) Edges

Figure 3.14: Cell viability on the wounded biochip
Live/dead staining of HDFs after wounding with Calecin AM-PI. The actuation of the membrane lead to the creation of the cell-free area shown in Figure (a). The dead cells are mostly present on the membrane (see Figure (b)), with only a few dead cells remaining in the wounded area. Figure (c) shows a close-up of the wound edge, where the majority of the cells remained alive. Scale = 200µm and 100µm, respectively.

Die approbierte gedruckte Originalversion dieser Diplomarbeit ist an der TU Wien Bibliothek verfügbar
The approved original version of this thesis is available in print at TU Wien Bibliothek.
TU WIEN Bibliothek Your knowledge hub

4. Discussion

A platform was designed that allows scientists to perform dynamic cultivation for biology experiments on microfluidic devices to facilitate mechanobiological research. The designed platform provides a functional and accessible solution to control a solenoid manifold at low cost.

The mechanobiological research interfaces biology and engineering by studying the effects of the physical environment on biological responses [85]. The physical stimulation often relies on a pneumatic infrastructure to relay pressure to and from solenoid valves to a cell-culture device. An infrastructure to relay pressure to and from solenoid valves to a device. The application fields for a pneumatic platform are not limited to mechanobiological research. The main concept of actuating an elastomeric membrane is common for microfluidic devices. While actuation of flexible membranes is vital to emulate organ functions in organ-on-a-chip devices, existent peripheral equipment is often bulky, expensive, and requires trained operators.

The platform designed within this thesis significantly advances platform flexibility and versatility compared to current systems that only provide constant and/or cyclic pressure by including a pneumatic peristaltic pump and a small vacuum chamber. But also including a pneumatic peristaltic pump and a small vacuum (generated with an inline vacuum ejector). Offering facilitation of the experimental setup at a low price was a key priority during the design process. A material price of under 100 € was rendered possible by using commercially available materials and purposely reduce the number of valves. This is approximately one-fifth of the price of any custom-built equivalent [38, 60–62].

The platform can easily be adapted to fit specific requirements of the user by using readily available components. All parts are interchangeable, from the electronics to the solenoid valves. The user is given a choice regarding the interface. Three different ways to control the platform were implemented. This allows every user the best possible experience, because the UI can be chosen depending on the users needs. For simple tasks a graphical user interface was designed, which allows for opening and closing of the valves by a button press, but requires a PC connection. The integrated UI consists of an LCD and rotary encoder combination. The LCD offers

Die approbierte gedruckte Originalversion dieser Diplomarbeit ist an der TU Wien Bibliothek verfügbar
The approved original version of this thesis is available in print at TU Wien Bibliothek.
TU Bibliothek Your knowledge hub WIEN

a graphical display of information at a low cost, with the added benefit of not relying on a physical touch as input. This UI was intentionally designed for a laboratory application. As gloves are mandatory in a laboratory, a touchscreen may become an unreliable input source. The rotary encoder allows the user to control the menu displayed on the LCD and thereby selecting the program and valves. By pressing the rotary encoder, the item gets selected and the program runs accordingly. The advanced control method may be utilized with the serial monitor of the Arduino IDE.

This platform improves upon existing devices with extended modularity, a smaller footprint, and a lower material price. Commercial bioreactors are often big in size; thus, it has been a priority during the design stage to minimize the footprint of the platform to fit the limited available lab space. The compact footprint is a direct result of limiting the number of available valves to eight. Which is useful as it is seldom necessary to control more than eight valves at a time. Nonetheless a design for a upscaled version has been made. Testing and characterization of this upscaled version is planned to be performed in the future.

Downsizing enables low cost high-throughput screening in contrast to regular sized bioreactors. The experiment presented could be performed with four chips (with eight chambers each) simultaneously. Consequently, a smaller platform reduces power consumption and space requirements while increasing portability. Considering the smaller sample sizes, smaller volumes of reagents are needed. Thus, reducing cost and minimizing waste. Which is especially important when working with hazardous biological materials [86].

The housing of the platform was custom designed and manufactured with an FDM printer. This is not only an extremely cheap but also allows fast manufacturing of design iterations. Using fitted joints as the main connection between the parts facilitates a straightforward assembly/disassembly of the platform without any tools. However, the current design can still be improved by increasing wall thickness or changing printing material to increase platform robustness. Bending may occur in case of extensive heat generation or a high force impact. This can be avoided by either thicken the walls or change the filament to ABS which has a higher melting point and is tougher than PLA.

Considering the electronics, an alternative for the microcontroller board may be considered in the future. An option would be a custom printed circuit board, which would also allow for integration of additional features such as Wi-Fi or Bluetooth. As the goal of this thesis was to provide a working prototype, it seemed reasonable to use an existing microcontroller board and shield, which offers not only a physical programmable circuit board, but also the integrated development environment. It would be interesting to characterize the circuit further regarding power consumption and valve opening time.

Die approbierte gedruckte Originalversion dieser Diplomarbeit ist an der TU Wien Bibliothek verfügbar
The approved original version of this thesis is available in print at TU Wien Bibliothek.
TU WIEN Bibliothek Your knowledge hub

The output pressure of the platform is currently controlled over pressure gauge of the main pressure line. While the device is stationed in the lab, connected to a main pressure line and pressure gauge, there was no need to implement a digital pressure regulator. However, to offer a fully portable all-in-one pneumatic control solution, a pump and pressure regulators must be integrated. It is planned to build a stand-alone version of the platform. This will include an integrated pump and a pressure control system. To control the pressure with the platform itself is the next step in development.

The platforms function was assessed with a miniaturized wound-healing biochip. This application was chosen because despite the wide-spread use of migration and wound healing assays, there is to date no satisfactory solution available that offers automated, highly reproducible wounds. This platform in combination with the biochip is capable of mechanically inducing circular cell-free areas in 2D cell-based models using mechanical trauma based on pneumatically actuated membranes. By cultivating a HDF monolayer in the biochip and connecting the biochip to the pneumatic platform, reproducible cell free areas were generated with high throughput.

The platform offers a compact multi-purpose solution to control microfluidic and mechanobiological devices while being compact in size and affordable. It has high potential for automatization, as it facilitates mechanobiological experimentation with little to no user intervention. The flexibility in hardware choice makes it trivial to adapt the system to different application needs.

Die approbierte gedruckte Originalversion dieser Diplomarbeit ist an der TU Wien Bibliothek verfügbar
The approved original version of this thesis is available in print at TU Wien Bibliothek.
TU WIEN Bibliothek Your knowledge hub

References

[1] K. H. Vining and D. J. Mooney, "Mechanical forces direct stem cell behaviour in development and regeneration," *Nature Reviews Molecular Cell Biology*, vol. 18, pp. 728–742, nov 2017.

[2] K. A. Jansen, D. M. Donato, H. E. Balcioglu, T. Schmidt, E. H. Danen, and G. H. Koenderink, "A guide to mechanobiology: Where biology and physics meet," *Biochimica et Biophysica Acta (BBA) - Molecular Cell Research*, vol. 1853, pp. 3043–3052, nov 2015.

[3] C. T. Lim, A. Bershadsky, and M. P. Sheetz, "Mechanobiology," *Journal of The Royal Society Interface*, vol. 7, apr 2010.

[4] Kaarj and Yoon, "Methods of delivering mechanical stimuli to organ-on-a-chip," *Micromachines*, vol. 10, p. 700, oct 2019.

[5] C. R. Jacobs, H. Huang, and of Ronald Y. Kwon, *Introduction to Cell Mechanics and Mechanobiology*. Taylor & Francis Inc, 2011.

[6] D. Mohammed, M. Versaevel, C. Bruyère, L. Alaimo, M. Luciano, E. Vercruysse, A. Procès, and S. Gabriele, "Innovative tools for mechanobiology: Unraveling outside-in and inside-out mechanotransduction," *Frontiers in Bioengineering and Biotechnology*, vol. 7, jul 2019.

[7] L. A. Low, C. Mummery, B. R. Berridge, C. P. Austin, and D. A. Tagle, "Organs-on-chips: into the next decade," *Nature Reviews Drug Discovery*, sep 2020.

[8] D. Huh, G. A. Hamilton, and D. E. Ingber, "From 3d cell culture to organs-on-chips," *Trends in Cell Biology*, vol. 21, pp. 745–754, dec 2011.

[9] L. C. Delon, A. Nilghaz, E. Cheah, C. Prestidge, and B. Thierry, "Unlocking the potential of organ-on-chip models through pumpless and tubeless microfluidics," *Advanced Healthcare Materials*, vol. 9, p. 1901784, apr 2020.

Die approbierte gedruckte Originalversion dieser Diplomarbeit ist an der TU Wien Bibliothek verfügbar
The approved original version of this thesis is available in print at TU Wien Bibliothek.
TU Bibliothek Your knowledge hub WIEN

[10] S. S. Nunes, J. W. Miklas, J. Liu, R. Aschar-Sobbi, Y. Xiao, B. Zhang, J. Jiang, S. Massé, M. Gagliardi, A. Hsieh, N. Thavandiran, M. A. Laflamme, K. Nanthakumar, G. J. Gross, P. H. Backx, G. Keller, and M. Radisic, "Biowire: a platform for maturation of human pluripotent stem cell–derived cardiomyocytes," *Nature Methods*, vol. 10, pp. 781–787, jun 2013.

[11] D. Huh, B. D. Matthews, A. Mammoto, M. Montoya-Zavala, H. Y. Hsin, and D. E. Ingber, "Reconstituting organ-level lung functions on a chip," *Science*, vol. 328, pp. 1662–1668, jun 2010.

[12] A. Marturano-Kruik, A. Villasante, K. Yaeger, S. Ambati, A. Chramiec, M. Raimondi, and G. Vunjak-Novakovic, "Biomechanical regulation of drug sensitivity in an engineered model of human tumor," *Biomaterials*, vol. 150, pp. 150–161, jan 2018.

[13] K. Ronaldson-Bouchard and G. Vunjak-Novakovic, "Organs-on-a-chip: A fast track for engineered human tissues in drug development," *Cell Stem Cell*, vol. 22, pp. 310–324, mar 2018.

[14] S. E. Park, A. Georgescu, and D. Huh, "Organoids-on-a-chip," *Science*, vol. 364, pp. 960–965, jun 2019.

[15] B. Zhang, A. Korolj, B. F. L. Lai, and M. Radisic, "Advances in organ-on-a-chip engineering," *Nature Reviews Materials*, vol. 3, pp. 257–278, aug 2018.

[16] T. D. Brown, "Techniques for mechanical stimulation of cells in vitro: a review," *Journal of Biomechanics*, vol. 33, pp. 3–14, jan 2000.

[17] V. D. Varner and C. M. Nelson, "Cellular and physical mechanisms of branching morphogenesis," *Development*, vol. 141, pp. 2750–2759, jul 2014.

[18] B. Kuehlmann, C. A. Bonham, I. Zucal, L. Prantl, and G. C. Gurtner, "Mechanotransduction in wound healing and fibrosis," *Journal of Clinical Medicine*, vol. 9, p. 1423, may 2020.

[19] J. Rosińczuk, J. Taradaj, R. Dymarek, and M. Sopel, "Mechanoregulation of wound healing and skin homeostasis," *BioMed Research International*, vol. 2016, pp. 1–13, 2016.

[20] D.-H. Kim, P. K. Wong, J. Park, A. Levchenko, and Y. Sun, "Microengineered platforms for cell mechanobiology," *Annual Review of Biomedical Engineering*, vol. 11, pp. 203–233, aug 2009.

[21] K. Yamamoto, T. Sokabe, T. Watabe, K. Miyazono, J. K. Yamashita, S. Obi, N. Ohura, A. Matsushita, A. Kamiya, and J. Ando, "Fluid shear stress induces differentiation of flk-1-positive embryonic stem cells into vascular endothelial cells in vitro," *American Journal of Physiology-Heart and Circulatory Physiology*, vol. 288, pp. H1915–H1924, apr 2005.

Die approbierte gedruckte Originalversion dieser Diplomarbeit ist an der TU Wien Bibliothek verfügbar
The approved original version of this thesis is available in print at TU Wien Bibliothek.
TU Bibliothek Your knowledge hub WIEN

[22] C. M. Metallo, M. A. Vodyanik, J. J. de Pablo, I. I. Slukvin, and S. P. Palecek, "The response of human embryonic stem cell-derived endothelial cells to shear stress," *Biotechnology and Bioengineering*, vol. 100, pp. 830–837, jan 2008.

[23] W. E. Thomas, E. Trintchina, M. Forero, V. Vogel, and E. V. Sokurenko, "Bacterial adhesion to target cells enhanced by shear force," *Cell*, vol. 109, pp. 913–923, jun 2002.

[24] C. A. Taylor and M. T. Draney, "Experimental and computational methods in cardiocascular fluid mechanics," *Annual Review of Fluid Mechanics*, vol. 36, pp. 197–231, jan 2004.

[25] J. E. Sosa-Hernández, A. M. Villalba-Rodríguez, K. D. Romero-Castillo, M. A. Aguilar-Aguila-Isaías, I. E. García-Reyes, A. Hernández-Antonio, I. Ahmed, A. Sharma, R. Parra-Saldívar, and H. M. N. Iqbal, "Organs-on-a-chip module: A review from the development and applications perspective," *Micromachines*, vol. 9, p. 536, oct 2018.

[26] S. Yasotharan, S. Pinto, J. G. Sled, S.-S. Bolz, and A. Günther, "Artery-on-a-chip platform for automated, multimodal assessment of cerebral blood vessel structure and function," *Lab on a Chip*, vol. 15, no. 12, pp. 2660–2669, 2015.

[27] E. Ergir, B. Bachmann, H. Redl, G. Forte, and P. Ertl, "Small force, big impact: Next generation organ-on-a-chip systems incorporating biomechanical cues," *Frontiers in Physiology*, vol. 9, oct 2018.

[28] F. Michielin, E. Serena, P. Pavan, and N. Elvassore, "Microfluidic-assisted cyclic mechanical stimulation affects cellular membrane integrity in a human muscular dystrophy in vitro model," *RSC Advances*, vol. 5, no. 119, pp. 98429–98439, 2015.

[29] H. Kamble, R. Vadivelu, M. Barton, K. Boriachek, A. Munaz, S. Park, M. Shiddiky, and N.-T. Nguyen, "An electromagnetically actuated double-sided cell-stretching device for mechanobiology research," *Micromachines*, vol. 8, p. 256, aug 2017.

[30] Y. Shao, X. Tan, R. Novitski, M. Muqaddam, P. List, L. Williamson, J. Fu, and A. P. Liu, "Uniaxial cell stretching device for live-cell imaging of mechanosensitive cellular functions," *Review of Scientific Instruments*, vol. 84, p. 114304, nov 2013.

[31] W. Tan, D. Scott, D. Belchenko, H. J. Qi, and L. Xiao, "Development and evaluation of microdevices for studying anisotropic biaxial cyclic stretch on cells," *Biomedical Microdevices*, vol. 10, pp. 869–882, jun 2008.

Die approbierte gedruckte Originalversion dieser Diplomarbeit ist an der TU Wien Bibliothek verfügbar
The approved original version of this thesis is available in print at TU Wien Bibliothek.
TU Bibliothek Your knowledge hub WIEN

[32] S. L. York, J. D. King, A. S. Pietros, B. Z. Newby, P. Sethu, and M. M. Saunders, "Development of a microloading platform for in vitro mechanotransduction studies," in *Mechanics of Biological Systems and Materials, Volume 7*, pp. 53–59, Springer International Publishing, jul 2014.

[33] B. Ladoux and R.-M. Mège, "Mechanobiology of collective cell behaviours," *Nature Reviews Molecular Cell Biology*, vol. 18, pp. 743–757, nov 2017.

[34] A. Shieh and K. Athanasiou, "Dynamic compression of single cells," *Osteoarthritis and Cartilage*, vol. 15, pp. 328–334, mar 2007.

[35] C. Moraes, Y. Sun, and C. A. Simmons, "(micro)managing the mechanical microenvironment," *Integrative Biology*, vol. 3, no. 10, p. 959, 2011.

[36] S.-H. Park, W. Y. Sim, B.-H. Min, S. S. Yang, A. Khademhosseini, and D. L. Kaplan, "Chip-based comparison of the osteogenesis of human bone marrow- and adipose tissue-derived mesenchymal stem cells under mechanical stimulation," *PLoS ONE*, vol. 7, p. e46689, sep 2012.

[37] G. S. Monfared, P. Ertl, and M. Rothbauer, "An on-chip wound healing assay fabricated by xurography for evaluation of dermal fibroblast cell migration and wound closure," *Scientific Reports*, vol. 10, oct 2020.

[38] B. Li, L. Li, A. Guan, Q. Dong, K. Ruan, R. Hu, and Z. Li, "A smartphone controlled handheld microfluidic liquid handling system," *Lab Chip*, vol. 14, no. 20, pp. 4085–4092, 2014.

[39] E. M. Darling and K. A. Athanasiou, "Articular cartilage bioreactors and bioprocesses," *Tissue Engineering*, vol. 9, pp. 9–26, feb 2003.

[40] S. Partap, N. A., and F. J., "Bioreactors in tissue engineering," in *Tissue Engineering*, InTech, mar 2010.

[41] E. B. Dolan, S. W. Verbruggen, and R. A. Rolfe, "Techniques for studying mechanobiology," in *Mechanobiology in Health and Disease*, pp. 1–53, Elsevier, 2018.

[42] R. Pörtner, S. Nagel-Heyer, C. Goepfert, P. Adamietz, and N. M. Meenen, "Bioreactor design for tissue engineering," *Journal of Bioscience and Bioengineering*, vol. 100, pp. 235–245, sep 2005.

[43] G. N. Bancroft, V. I. Sikavitsas, and A. G. Mikos, "Technical note: Design of a flow perfusion bioreactor system for bone tissue-engineering applications," *Tissue Engineering*, vol. 9, pp. 549–554, jun 2003.

[44] G. Vunjak-Novakovic, B. Obradovic, I. Martin, P. Bursac, R. Langer, and L. Freed, "Dynamic cell seeding of polymer scaffolds for cartilage tissue engineering," *Biotechnology Progress*, vol. 14, pp. 193–202, apr 1998.

Die approbierte gedruckte Originalversion dieser Diplomarbeit ist an der TU Wien Bibliothek verfügbar
The approved original version of this thesis is available in print at TU Wien Bibliothek.
TU Bibliothek Your knowledge hub WIEN

[45] D. W. Youngstrom, J. E. LaDow, and J. G. Barrett, "Tenogenesis of bone marrow-, adipose-, and tendon-derived stem cells in a dynamic bioreactor," *Connective Tissue Research*, vol. 57, pp. 454–465, mar 2016.

[46] D. W. Youngstrom, I. Rajpar, D. L. Kaplan, and J. G. Barrett, "A bioreactor system for in vitro tendon differentiation and tendon tissue engineering," *Journal of Orthopaedic Research*, vol. 33, pp. 911–918, apr 2015.

[47] A. Cochis, S. Grad, M. J. Stoddart, S. Farè, L. Altomare, B. Azzimonti, M. Alini, and L. Rimondini, "Bioreactor mechanically guided 3d mesenchymal stem cell chondrogenesis using a biocompatible novel thermo-reversible methylcellulose-based hydrogel," *Scientific Reports*, vol. 7, mar 2017.

[48] D. Lee, A. Erickson, T. You, A. T. Dudley, and S. Ryu, "Pneumatic microfluidic cell compression device for high-throughput study of chondrocyte mechanobiology," *Lab on a Chip*, vol. 18, no. 14, pp. 2077–2086, 2018.

[49] Y. Li, Y. Li, Q. Zhang, L. Wang, M. Guo, X. Wu, Y. Guo, J. Chen, and W. Chen, "Mechanical properties of chondrocytes estimated from different models of micropipette aspiration," *Biophysical Journal*, vol. 116, pp. 2181–2194, jun 2019.

[50] D. MartÍnez-Moreno, G. Jiménez, P. Gálvez-Martín, G. Rus, and J. Marchal, "Cartilage biomechanics: A key factor for osteoarthritis regenerative medicine," *Biochimica et Biophysica Acta (BBA) - Molecular Basis of Disease*, vol. 1865, pp. 1067–1075, jun 2019.

[51] P. Occhetta, A. Mainardi, E. Votta, Q. Vallmajo-Martin, M. Ehrbar, I. Martin, A. Barbero, and M. Rasponi, "Hyperphysiological compression of articular cartilage induces an osteoarthritic phenotype in a cartilage-on-a-chip model," *Nature Biomedical Engineering*, vol. 3, pp. 545–557, jun 2019.

[52] J. J. Wille, C. M. Ambrosi, and F. C.-P. Yin, "Comparison of the effects of cyclic stretching and compression on endothelial cell morphological responses," *Journal of Biomechanical Engineering*, vol. 126, pp. 545–551, oct 2004.

[53] A. J. Grodzinsky, M. E. Levenston, M. Jin, and E. H. Frank, "Cartilage tissue remodeling in response to mechanical forces," *Annual Review of Biomedical Engineering*, vol. 2, pp. 691–713, aug 2000.

[54] J. P. Halloran, S. Sibole, C. C. van Donkelaar, M. C. van Turnhout, C. W. J. Oomens, J. A. Weiss, F. Guilak, and A. Erdemir, "Multiscale mechanics of articular cartilage: Potentials and challenges of coupling musculoskeletal, joint, and microscale computational models," *Annals of Biomedical Engineering*, vol. 40, pp. 2456–2474, may 2012.

Die approbierte gedruckte Originalversion dieser Diplomarbeit ist an der TU Wien Bibliothek verfügbar
The approved original version of this thesis is available in print at TU Wien Bibliothek.
TU Bibliothek Your knowledge hub WIEN

[55] W. Wang, Y. Wan, T. Fu, T. Zhou, X. Tang, H. Wu, C. Liu, and M. Jagodzinski, "Effect of cyclic compression on bone marrow mesenchymal stromal cells in tissue engineered cartilage scaffold," *Journal of Biomedical Materials Research Part A*, vol. 107, pp. 1294–1302, feb 2019.

[56] O. T. Guenat and F. Berthiaume, "Incorporating mechanical strain in organs-on-a-chip: Lung and skin," *Biomicrofluidics*, vol. 12, p. 042207, jul 2018.

[57] F. I. Corporation, "Fluid shear stress flow systems," Apr. 2020. Retrieved on 22.04.2020 form URL.

[58] Strex, "Cell stretching systems," Apr. 2020. Retrieved on 22.04.2020.

[59] T. Instruments, "Biodynamic 5100," Apr. 2020. Retrieved on 22.04.2020 form .

[60] C. Watson and S. Senyo, "All-in-one automated microfluidics control system," *HardwareX*, vol. 5, p. e00063, apr 2019.

[61] J. A. White and A. M. Streets, "Controller for microfluidic large-scale integration," *HardwareX*, vol. 3, pp. 135–145, apr 2018.

[62] K. Brower, R. R. Puccinelli, C. J. Markin, T. C. Shimko, S. A. Longwell, B. Cruz, R. Gomez-Sjoberg, and P. M. Fordyce, "An open-source, programmable pneumatic setup for operation and automated control of single- and multi-layer microfluidic devices," *HardwareX*, vol. 3, pp. 117–134, apr 2018.

[63] C. Zhang, D. Xing, and Y. Li, "Micropumps, microvalves, and micromixers within PCR microfluidic chips: Advances and trends," *Biotechnology Advances*, vol. 25, pp. 483–514, sep 2007.

[64] V. Lecault, A. K. White, A. Singhal, and C. L. Hansen, "Microfluidic single cell analysis: from promise to practice," *Current Opinion in Chemical Biology*, vol. 16, pp. 381–390, aug 2012.

[65] H. Q. Nguyen, K. Brower, B. Harink, B. Baxter, K. S. Thorn, and P. M. Fordyce, "Peptide library synthesis on spectrally encoded beads for multiplexed protein/peptide bioassays," in *Microfluidics, BioMEMS, and Medical Microsystems XV* (B. L. Gray and H. Becker, eds.), SPIE, feb 2017.

[66] R. Gómez-Sjöberg, A. A. Leyrat, D. M. Pirone, C. S. Chen, and S. R. Quake, "Versatile, fully automated, microfluidic cell culture system," *Analytical Chemistry*, vol. 79, pp. 8557–8563, nov 2007.

[67] M. A. Unger, "Monolithic microfabricated valves and pumps by multilayer soft lithography," *Science*, vol. 288, pp. 113–116, apr 2000.

Die approbierte gedruckte Originalversion dieser Diplomarbeit ist an der TU Wien Bibliothek verfügbar
The approved original version of this thesis is available in print at TU Wien Bibliothek.
TU Bibliothek Your knowledge hub WIEN

[68] T. Thorsen, "Microfluidic large-scale integration," *Science*, vol. 298, pp. 580–584, sep 2002.

[69] S. E. Hulme, S. S. Shevkoplyas, and G. M. Whitesides, "Incorporation of prefabricated screw, pneumatic, and solenoid valves into microfluidic devices," *Lab Chip*, vol. 9, no. 1, pp. 79–86, 2009.

[70] W. H. Grover, R. H. C. Ivester, E. C. Jensen, and R. A. Mathies, "Development and multiplexed control of latching pneumatic valves using microfluidic logical structures," *Lab on a Chip*, vol. 6, no. 5, p. 623, 2006.

[71] W. Zhang, S. Lin, C. Wang, J. Hu, C. Li, Z. Zhuang, Y. Zhou, R. A. Mathies, and C. J. Yang, "PMMA/PDMS valves and pumps for disposable microfluidics," *Lab on a Chip*, vol. 9, no. 21, p. 3088, 2009.

[72] W. H. Grover, A. M. Skelley, C. N. Liu, E. T. Lagally, and R. A. Mathies, "Monolithic membrane valves and diaphragm pumps for practical large-scale integration into glass microfluidic devices," *Sensors and Actuators B: Chemical*, vol. 89, pp. 315–323, apr 2003.

[73] D. Industry, "Choosing the right solenoid valve," May 2020. Retrieved form URL on 13.05.20.

[74] EWP, "Introduction to solenoid valves," May 2020. Retrived on 05.05.20 from URL.

[75] EWP, "Valves guide," May 2020. Retrived on 05.05.20 from URL.

[76] B. U. L. F. C. Center, "What is a solenoid valve and how does it work?," May 2020. Retrieved form URL on 12.05.20.

[77] V. Narayanamurthy, Z. E. Jeroish, K. S. Bhuvaneshwari, P. Bayat, R. Premkumar, F. Samsuri, and M. M. Yusoff, "Advances in passively driven microfluidics and lab-on-chip devices: a comprehensive literature review and patent analysis," *RSC Advances*, vol. 10, no. 20, pp. 11652–11680, 2020.

[78] D. J. Laser and J. G. Santiago, "A review of micropumps," *Journal of Micromechanics and Microengineering*, vol. 14, pp. R35–R64, apr 2004.

[79] B. Zhao, X. Cui, W. Ren, F. Xu, M. Liu, and Z.-G. Ye, "A controllable and integrated pump-enabled microfluidic chip and its application in droplets generating," *Scientific Reports*, vol. 7, sep 2017.

[80] Z. Li, S. Y. Mak, A. Sauret, and H. C. Shum, "Syringe-pump-induced fluctuation in all-aqueous microfluidic system implications for flow rate accuracy," *Lab on a Chip*, vol. 14, no. 4, p. 744, 2014.

Die approbierte gedruckte Originalversion dieser Diplomarbeit ist an der TU Wien Bibliothek verfügbar
The approved original version of this thesis is available in print at TU Wien Bibliothek.
TU Bibliothek Your knowledge hub WIEN

[81] L. Yobas, K.-C. Tang, S.-E. Yong, and E. K.-Z. Ong, "A disposable planar peristaltic pump for lab-on-a-chip," *Lab on a Chip*, vol. 8, no. 5, p. 660, 2008.

[82] SMC, *Vacuum Ejector Box Style (Built-in Silencer)/Body Ported Style Series ZH*. smc. ZH05BS-06-06.

[83] Arduino, "Arduino uno rev3," Dec. 2020. Retrieved on 20.12.2020 form URL.

[84] T. Instruments, "Uln2803a darlington transistor arrays." Datasheet, Jan. 2021. Retrieved on 22.04.2020 form URL.

[85] S. Baratchi, K. Khoshmanesh, C. D. Cox, and G. A. Gomez, "Editorial: Mechanobiology: Emerging tools and methods," *Frontiers in Bioengineering and Biotechnology*, vol. 8, apr 2020.

[86] G. Pasirayi, V. Auger, S. M. Scott, P. K. Rahman, M. Islam, L. O'Hare, and Z. Ali, "Microfluidic bioreactors for cell culturing: A review," *Micro and Nanosystemse*, vol. 3, pp. 137–160, jul 2011.

Die approbierte gedruckte Originalversion dieser Diplomarbeit ist an der TU Wien Bibliothek verfügbar
The approved original version of this thesis is available in print at TU Wien Bibliothek.
TU Bibliothek Your knowledge hub WIEN

A. Appendix

A.1 Design for a upscaled platform

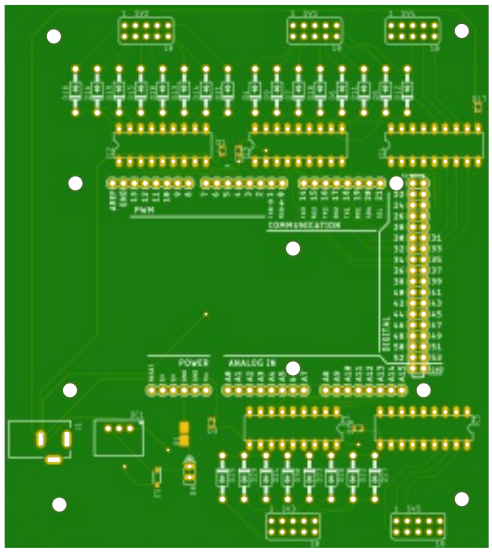

(a) Frontside

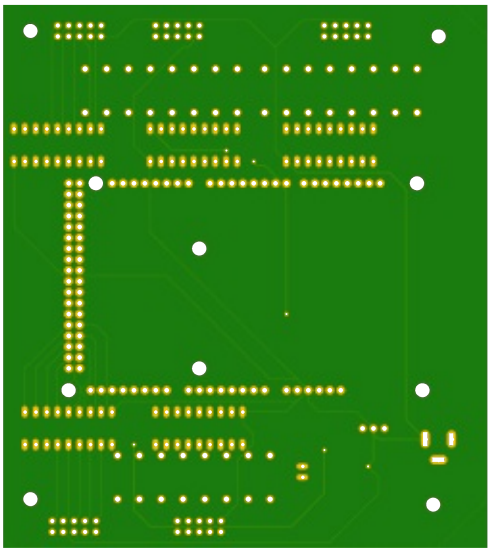

(b) Backside

PCB Design

Die approbierte gedruckte Originalversion dieser Diplomarbeit ist an der TU Wien Bibliothek verfügbar
The approved original version of this thesis is available in print at TU Wien Bibliothek.
TU WIEN Bibliothek Your knowledge hub

Die approbierte gedruckte Originalversion dieser Diplomarbeit ist an der TU Wien Bibliothek verfügbar
The approved original version of this thesis is available in print at TU Wien Bibliothek.

A.1.1 Schematic

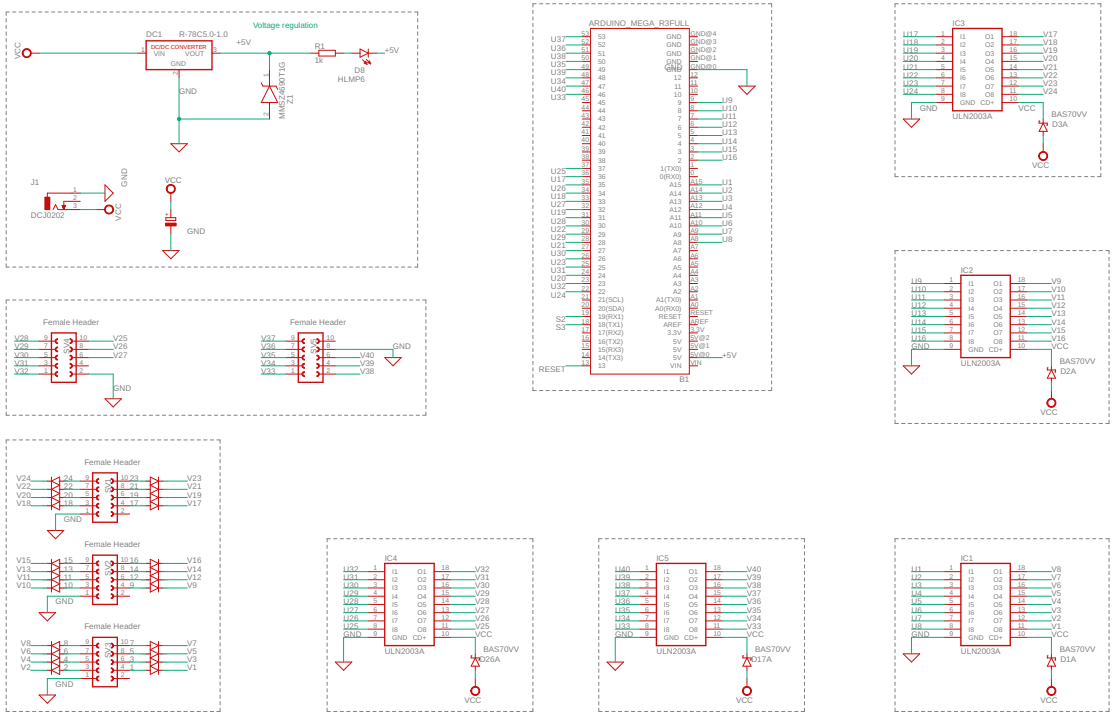

TU Bibliothek
Your knowledge hub
WIEN

Die approbierte gedruckte Originalversion dieser Diplomarbeit ist an der TU Wien Bibliothek verfügbar
The approved original version of this thesis is available in print at TU Wien Bibliothek.

A.2 Parts list

Table A.1: Part List for Upscaled Version

Part	Value	Device	Package	Description
B1	Arduino Mega	Arduino Mega	Full_Arduino_Mega	Arduino Mega 2560
D1	BAS70VV	BAS70VV	SOT666	Silicon Schottky Diodes
D2	BAS70VV	BAS70VV	SOT666	Silicon Schottky Diodes
D3	BAS70VV	BAS70VV	SOT666	Silicon Schottky Diodes
D4	1N4004	1N4004	DO41-10	Diode
D5	1N4004	1N4004	DO41-11	Diode
D6	1N4004	1N4004	DO41-12	Diode
D7	1N4004	1N4004	DO41-13	Diode
D8	HLMP6	HLMP6	HLMP6	LED
D9	1N4004	1N4004	DO41-10	Diode
D10	1N4004	1N4004	DO41-11	Diode
D11	1N4004	1N4004	DO41-12	Diode

Die approbierte gedruckte Originalversion dieser Diplomarbeit ist an der TU Wien Bibliothek verfügbar
The approved original version of this thesis is available in print at TU Wien Bibliothek.

Table A.1 continued from previous page

D12	1N4004	1N4004	DO41-13	Diode
D13	1N4004	1N4004	DO41-10	Diode
D14	1N4004	1N4004	DO41-11	Diode
D15	1N4004	1N4004	DO41-12	Diode
D16	1N4004	1N4004	DO41-13	Diode
D17	BAS70VV	BAS70VV	SOT666	Silicon Schottky Diodes
D18	1N4004	1N4004	DO41-11	Diode
D19	1N4004	1N4004	DO41-12	Diode
D20	1N4004	1N4004	DO41-13	Diode
D21	1N4004	1N4004	DO41-14	Diode
D22	1N4004	1N4004	DO41-15	Diode
D23	1N4004	1N4004	DO41-16	Diode
D24	1N4004	1N4004	DO41-17	Diode
D25	1N4004	1N4004	DO41-18	Diode
D26	BAS70VV	BAS70VV	SOT666	Silicon Schottky Diodes

Die approbierte gedruckte Originalversion dieser Diplomarbeit ist an der TU Wien Bibliothek verfügbar
The approved original version of this thesis is available in print at TU Wien Bibliothek.

Table A.1 continued from previous page

D27	1N4004	1N4004	DO41-16	Diode
D28	1N4004	1N4004	DO41-17	Diode
D29	1N4004	1N4004	DO41-18	Diode
D30	1N4004	1N4004	DO41-18	Diode
DC1	R-78C5.0-1.0	R-78C5.0-1.0	SIP3	DC/DC-Converter
IC1	ULN2003A	ULN2003A	DIL18	Driver Array
IC2	ULN2003A	ULN2003A	DIL19	Driver Array
IC3	ULN2003A	ULN2003A	DIL20	Driver Array
IC4	ULN2003A	ULN2003A	DIL21	Driver Array
IC5	ULN2003A	ULN2003A	DIL22	Driver Array
J1	DCJ0202	DCJ0202	DCJ0202	DC Power Jack
R1	1k	SMK	SMK	SMD Shunt Resistor
SV1	Female Header	FE05-2	FE05-2	Female Header
SV2	Female Header	FE05-2	FE05-2	Female Header
SV3	Female Header	FE05-2	FE05-2	Female Header

Die approbierte gedruckte Originalversion dieser Diplomarbeit ist an der TU Wien Bibliothek verfügbar
The approved original version of this thesis is available in print at TU Wien Bibliothek.

Table A.1 continued from previous page

SV4	Female Header	FE05-2	FE05-2	Female Header
SV5	Female Header	FE05-2	FE05-2	Female Header
Z1	MMSZ4690T1G	MMSZ4690T1G	SOD3716X135N	ON Semiconductor MMSZ4690T1G Zener Diode